Synthesis of carbon nanotube composite membranes for catalytic wet peroxide oxidation of emerging contaminants

Paulo Cesar Zadra Filho

State-of-the-Art submitted to

Escola Superior de Tecnologia e Gestão

Instituto Politécnico de Bragança

Master degree in

Chemical Engineering

within the scope of the double diploma with

Universidade Tecnológica Federal do Paraná Câmpus Ponta Grossa

Supervisors:

Prof. Dr. Helder Teixeira Gomes

Prof[a]. Dra. Juliana Martins Teixeira de Abreu Pietrobelli

Bragança, Portugal

2024

ACKNOWLEDGEMENTS

Since the beginning of this project, I have been fortunate to receive support from many people who were essential to my personal development and the completion of this work. I am deeply grateful to my family and friends, who have always supported me.

I would like to express my special thanks to my advisors, Professor Dr. Helder Teixeira Gomes from the Polytechnic Institute of Bragança (IPB), and Professor Dr. Juliana Martins Teixeira de Abreu Pietrobelli from the Federal University of Technology - Paraná (UTFPR-PG), for their constant support, valuable guidance, and trust. I also extend my gratitude to doctoral students Adriano dos Santos Silva, Fernanda Fontana Roman, and Ana Paula Ferreira da Silva, who generously shared their knowledge and time, greatly contributing to my learning and growth.

I am grateful for having participated in a project supported by the Mountain Research Center (CIMO), and I would like to extend my appreciation to Professor Dr. Paula Plasencia (IPB-CIMO), who welcomed, guided, and introduced me to the research group when I first joined the double degree program (DD) at IPB. I also express my gratitude for the DD agreement between IPB and UTFPR-PG, as well as for the dedication of those who make this partnership possible, especially Professor Dr. Juliana Martins Teixeira de Abreu Pietrobelli, who is responsible for the Internationalization Activities (PRAInt) in the Chemical Engineering program.

Finally, I thank my supervisors and mentors from the innovation internship program, Augusto Oliveira and Marco Festas, for their flexibility, support, and the opportunity to advance in this master's project while working at C-Pack Creative Packaging Portugal.

Abstract

Global challenges of water contamination and plastic waste management demand innovative solutions to address emerging contaminants (CECs) and promote sustainable practices. This dissertation investigates the development and testing of catalytic nanocomposite membranes (CNMs), synthesized from polyvinylidene fluoride (PVDF), polyvinylpyrrolidone (PVP), and carbon nanotubes (CNTs) with the potential to be derived from plastic solid waste (PSW). These CNMs were evaluated for their potential to degrade sulfamethoxazole (SMX), an antibiotic found in water sources worldwide, through catalytic wet peroxide oxidation (CWPO) in a continuous filtration system. Among AOPs, CWPO has demonstrated potential for the efficient decomposition of organic pollutants. CNTs, synthesized via catalytic chemical vapor deposition (CCVD) using iron oxide supported on alumina as a metal substrate, were incorporated into polymeric membranes to provide them with degradation capabilities. Experimental analysis included the synthesis of CNMs via phase inversion. Characterization was conducted using scanning electron microscopy (SEM), textural properties, overall membrane porosity, largest pore size, hydrophobicity and hydrophilicity, morphology, and thermal decomposition. The membranes were tested in CWPO-enhanced filtration systems to evaluate their SMX degradation potential. The results demonstrated that CNMs with incorporated CNTs significantly improved SMX removal, achieving up to 90% efficiency under continuous flow conditions, with a pollutant degradation mass of up to 2551 mg m^{-2} h^{-1}. The CNMs exhibited enhanced hydrogen peroxide decomposition (over 80%) and uniform CNT distribution, as verified by SEM analysis, with no significant iron leaching during the CWPO-enhanced filtration processes. These findings suggest that CNT-based membranes can serve as efficient catalysts in wastewater treatment, facilitating both filtration and oxidative degradation of CECs.In conclusion, this research advances the field of water purification by demonstrating the effectiveness of CNMs in CWPO applications. It reinforces the role of plastic waste recovery in the development of functional nanocomposite membranes, supporting the upcycling of PSWs, contributing to the circular economy, and promoting environmental sustainability and water decontamination.

Key words: Catalytic nanocomposite membranes; Carbon nanotubes; Plastic waste; Upcycling; Catalytic oxidation with hydrogen peroxide; Sulfamethoxazole.

Resumo

Os desafios globais de contaminação da água e gestão de resíduos plásticos exigem soluções inovadoras para enfrentar contaminantes emergentes (CECs) e promover práticas sustentáveis. Esta dissertação investiga o desenvolvimento e teste de membranas nanocompósitas catalíticas (CNMs), sintetizadas a partir de fluoreto de polivinilideno (PVDF), polivinilpirrolidona (PVP) e nanotubos de carbono (CNTs) com potencial para serem feitos de resíduos sólidos plásticos (PSW). Essas CNMs foram avaliadas por seu potencial de degradar sulfametoxazol (SMX), um antibiótico encontrado em fontes de água em todo o mundo, por meio da oxidação catalítica com peróxido (CWPO) em um sistema contínuo de filtração. Entre os AOPs, a CWPO tem demonstrado potencial para a decomposição eficiente de poluentes orgânicos. Os CNTs, sintetizados via deposição química a vapor catalítica (CCVD) usando óxido de ferro suportado em alumina como substrato metálico, foram incorporados em membranas poliméricas para atribuir a elas capacidades de degradação. A análise experimental incluiu a síntese de CNMs por inversão de fase. A caracterização foi feita utilizando microscopia eletrônica de varredura (SEM), propriedades texturais, porosidade total da membrana, maior tamanho de poro, hidrofobicidade e hidrofilicidade, morfologia e decomposição térmica. As membranas foram testadas em sistemas de filtração intensificados com CWPO para avaliar sua capacidade de degradar SMX. Os resultados demonstraram que CNMs com CNTs incorporados melhoraram significativamente a remoção de SMX, alcançando até 90% de eficiência em condições de fluxo contínuo, com uma degradação de massa de poluentes de até 2551 mg m^{-2} h^{-1}. As CNMs exibiram maior decomposição de peróxido de hidrogênio (acima de 80%) e distribuição uniforme de CNTs, conforme verificado pela análise de SEM, sem lixiviação significativa de ferro durante as filtrações intensificadas por CWPO. Esses achados sugerem que membranas à base de CNTs podem servir como catalisadores eficientes no tratamento de águas residuais, facilitando tanto a filtração quanto a degradação oxidativa de CECs. Em conclusão, esta pesquisa avança no campo da purificação da água ao demonstrar a eficácia das CNMs na CWPO. Ela reforça o papel da recuperação de resíduos plásticos no desenvolvimento de membranas nanocompósitas funcionais, apoiando o conceito de upcycle de PSWs, contribuindo para a economia circular, promovendo a sustentabilidade ambiental e a descontaminação da água.

Palavras chave: Membranas nanocompósitas catalítica; Nanotubos de carbono; resíduos plásticos; upcycling; Oxidação catalítica com peróxido de hidrogénio; sulfametoxazol.

TABLE OF CONTENTES

LIST OF FIGURES

LIST OF TABLES

LIST OF ABBREVIATION

AOP	Advanced oxidation process
APA	United States Environmental Protection Agency
ASTM	American Society for Testing and Materials
ASW	artificial sweeteners
BPA	Bisphenol-A
BPCNT	Membranes with buckypaper CNTs
CAS	American Chemical Society
CCPSCNT	Membranes with dispersed CNTs
CCVD	Catalytic chemical vapor deposition
CECs	Contaminants of emerging concern
CMR	Catalytic membrane reactor
CNM	Catalytic nanocomposite membrane
CNT	Carbon nanotubes
CVD	Chemical vapor deposition
CWPO	Wet peroxide catalytic oxidation
DBP	Disinfection by-products
DDT	Dichlorodiphenyltrichloroethane
DQAA	Water Framework Directive
DTG	Differential thermogravimetry
EC	European Commission
ECs	Emerging contaminants
EDC	Endocrine disrupting chemicals
EE2	α-ethinylestradiol
EFSA	European Food Safety Authority
EP	Emerging pollutant
EU	European Union
FR	Flame retardants
FT-IR	Fourier transform infrared spectroscopy
HDPE	High Density Polyethylene
LDPE	Low density polyethylene
LDPE	Low Density Polyethylene
CNMS	Catalytic nanocomposite membranes
MONPs	Metal oxide nanoparticles
MP	Micro pollutants
MSW	Municipal solid waste
MWNTs	Multi-walled carbon nanotubes
OPEs	Organophosphorus esters
PAEs	Phthalic acid
PE	Polyethylene
PECVD	Plasma enhanced chemical vapor deposition
PET	Polyethylene terephthalate
PFCs	Perfluorinated organic compounds
PFOA	Perfluorooctanoic acid
PFOS	Perfluorooctane sulfonic acid
PM	Polymeric membrane
PNM	Polymer nanocomposite membrane
POP	Persistent organic pollutant
PP	Polypropylene
PPCP	Pharmaceutical and personal care product
PS	Polystyrene
PSW	Solid plastic waste
PTFE	Polytetrafluoroethylene
PUR	Polyurethane
PVC	Polyvinyl chloride
PVD	Physical vapor deposition
PVDF	Polyvinylidene fluoride
PWR	Recovery of plastic waste
SEM	Scanning Electron Microscopy
TEM	Transmission Electron Microscopy
SMX	Sulfamethoxazole
SWNTs	Single-walled carbon nanotubes
TG	Thermogravimetric
TOC	Total Organic Carbon
TPD	Temperature-programmed desorption
VACNT	Vertically aligned CNT membranes
WCA	Water contact angle
WWTPs	Wastewater treatment plants

1 INTRODUCTION

Humanity faces significant challenges in mitigating its environmental impacts, such as the overconsumption of natural resources and uncontrolled waste generation, emphasizing the need for sustainable practices in the coming decade (Jehanno et al., 2022). In this context, developing technologies for better water management, including methods to safely reuse treated wastewater and repurpose plastic residues, represents a critical advance (Liu et al., 2017).For instance, converting plastic waste into carbon nanotubes (CNTs) offers a promising route for upcycling solid plastic waste (PSW) and enhancing water filtration through nanocomposite membranes (Y. S. Zhang et al., 2021).

Previous studies on CNTs from plastic residues have largely focused on feasibility, process optimization, and diverse applications, with fewer efforts dedicated to developing CNTs for filtration intensification. A prevalent method for producing CNTs is catalytic chemical vapor deposition (CCVD) on metal substrates such as iron or cobalt. (Diaz de Tuesta et al., 2023).

Magnetic nanostructured carbon materials have drawn interest, especially for processes like Fenton reactions and catalytic wet peroxide oxidation (CWPO), due to their catalytic efficiency and potential for in-situ magnetic separation (Silva et al., 2023). CWPO, applied in wastewater treatment, oxidizes organic pollutants using hydrogen peroxide and a suitable catalyst (Santos Silva et al., 2019).

Polymeric membranes (PMs) have long been used in water treatment (Pendergast & Hoek, 2011), but integrating catalysts into these membranes for advanced oxidation processes (AOPs) is a recent development. Some studies using carbon nanocomposites, such as CNTs, have shown promising results in enhancing filtration and efficiently decomposing contaminants of emerging concern (CECs) (C. Chen et al., 2023).

This research combines these efforts, exploring the filtration intensification to CECs removal via CWPO and the integration of plastic residues into nanocomposites (Ribeiro et al., 2022; Diaz de Tuesta et al., 2023; Silva et al., 2023; Roman et al., 2023). It promotes PSW upcycling and shows one strategy to improve wastewater treatment efficiency. The study aims to develop and test catalytic nanocomposite membranes (CNMs) made of polyvinylidene fluoride (PVDF), polyvinylpyrrolidone (PVP), and CNTs. These membranes will be tested for their efficiency in degrading sulfamethoxazole (SMX) using CWPO in a continuous flow system to evaluate the characteristics and the filtration intensification of the membranes produced.

2 OBJECTIVES AND SCOPE

The main objective of this work is to develop different catalytic nanocomposite membranes (CNMs) and test their respective potential for the degradation of contaminants of emerging concern (CECs) in a continuous flow system by catalytic wet peroxide oxidation (CWPO) to improve filtration of the pollutants. The micropollutant selected for this experimental research was the antibiotic sulfamethoxazole (SMX) found in surface and ground waters worldwide. For this purpose, CNMs will be produced by incorporating carbon nanotubes (CNTs) on a polymeric membrane matrix. These nanomaterials are made from low-density polyethylene (LDPE), a polyolefin that was chosen as a model polymer from plastic solid waste (PSW). The CNT growth involves catalytic chemical vapor deposition (CCVD), using iron oxide supported on alpha alumina (IO/Al_2O_3) as a metal substrate. The aim is to evaluate the physicochemical differences between the produced polymeric catalytic membranes, to investigate their respective potentials to filtrate and for mineralizing CECs, to demonstrate that these membranes have the potential to be upcycling products to insert PSWs in a circular economy, performing plastic solid waste recovery (PSW) upcycling and enhancing the application of CNTs in CWPO.

3 STATE OF THE ART

3.1 Water contamination and reuse

One of the global concerns is the scarcity of drinking water. It is estimated that by 2050, about 50% of the world's population will be in a situation of water stress (Liu et al., 2017). Compounding this problem is the contamination of water resources associated with anthropogenic activities such as urban, industrial, livestock and agricultural population growth. It is estimated that 30% of the world's population will not have access to quality drinking water within this decade, making it imperative to develop technologies to mitigate this situation (World Health Organization, 2023).

The most common contaminants in water matrices that have received attention in recent decades are those derived from pharmaceuticals and plastics. Many pharmaceuticals people ingest are excreted into the sewerage system and do not receive proper treatment. Similarly, some plastic waste is not correctly disposed of and ends up contaminating soil, air, and water resources (Wilkinson et al., 2017; Xu et al., 2021).

Therefore, developing technologies to treat and degrade these pollutants is essential to safely reuse water resources and enable a sustainable consumption cycle. In addition, it is worth developing methods to reduce the improper disposal of materials that cause these pollutants, such as plastics and pharmaceuticals, by promoting collection and recycling, with plastic waste still capable of being recovered and incorporated into a circular economy (Rout et al., 2021).

3.2 Contaminants of emerging concern (CECs)

Contaminants of emerging concern (CECs) or emerging contaminants (ECs) are synthetic or natural chemical substances, mostly organic compounds of various origins, that can be found in soil, air or water in a wide range of concentrations, from parts per trillion (ppt or ng/L) to parts per million (ppm or mg/L), and have some adverse effect on the environment and living organisms. In addition, they are not commonly monitored or removed from the environment (Schnoor, 2003;Sauvé & Desrosiers, 2014)

CECs cover a wide range of chemicals. According to the OW/ORD Emerging Contaminants Workgroup (2008), the U.S. Environmental Protection Agency (EPA) published the Aquatic Life Criteria for Contaminants of Emerging Concern in 2008, defining an emerging contaminant as a chemical substance or material that has been identified as a potential or actual threat to human health and the environment. In doing so, it classified some of these emerging contaminants, some of which include:

Pharmaceuticals and personal care products (PPCPs), which include a broad group of prescription and over-the-counter drugs and cosmetics, such as antidepressants, blood pressure medications, analgesics, bactericides, synthetic fragrances, and sunscreens.

- Persistent organic pollutants (POPs), such as polybrominated diphenyl ethers (PBDEs) found in flame retardants (FRs), coating foams and plastics, also include perfluorinated organic compounds (PFCs).
- Animal health products can include antimicrobials, antibiotics, antifungals, growth promoters and hormones.
- Endocrine disrupting chemicals (EDCs), which include synthetic or natural estrogens such as 17α-ethynylestradiol and testosterone, androgens such as trenbolone and other natural hormones, as well as organochlorine pesticides and alkylphenols.
- Nanomaterials, such as nanometer-scale particulate titanium dioxide.

In addition, other CECs have been identified from various of sources: landfill leachate, illicit drugs, artificial sweeteners, disinfection byproducts, UV filters, microplastics, and others. Some of these compounds are composed of complex molecules that resist some traditional degradation alternatives. As a result, the degradation process of these CECs can produce intermediates that are in some cases even more toxic and reactive than the original compounds (Yadav et al., 2021).

3.2.1 CECs in the environment

Most CECs are of anthropogenic origin and are currently found in the atmosphere, various soil types, surface water, groundwater and drinking water. On the other hand, they are found in higher concentrations in the effluents of wastewater treatment plants (WWTPs). They are also found in various types of wastewaters: domestic, industrial, hospital, landfill runoff or leachate, and water used in agriculture or for livestock. This widespread presence of CECs is due to their potential for dispersal, the accumulation of some contaminants at trophic levels, and the lack of identification for specific treatment and degradation of CECs. There is no low-cost, safe generation of toxic intermediates or comprehensive technologies to degrade a variety of CECs simultaneously. The harmful effects of CECs on the environment have been widely studied, and there is still uncertainty about the real effect of some substances, but it is known that most of these compounds are lipophilic substances and cause bioaccumulation in living beings, death and deformation of microorganisms, distortion of the nitrogen cycle, methanogenesis,

reduction of sulfates and interference in the soil nutrient cycle. Another problem would be the selection of microorganisms that are more resistant to existing drugs, mainly caused by antibiotic compounds (Luo et al., 2014; Rasheed et al., 2019; Prasannamedha & Kumar, 2020).

3.2.2 Effects on the health of living organisms

One of the current concerns motivating the development of new research is the effects of various CECs on the health of living organisms. Through prolonged exposure and ingestion of toxic levels, the relationship between many emerging pollutants and alterations in health, biological development and reproduction of living beings is becoming evident. This occurs even at low concentrations of these compounds, on the order of micrograms and nanograms per liter. For example, surfactant micropollutants, some of which act as EDCs, alter the body's ability to synthesize, metabolize, and transport endogenous hormones. This adversity is also due to the ability of some EDCs to act as exogenous substances that mimic and antagonize the endogenous substances of living organisms, causing hormonal dysregulation. In addition, other EDCs are known to act as carcinogens, such as plasticizers, neurotoxic substances, such as pesticides, and bioaccumulators, such as flame retardants (Feng et al., 2023).

Table 1 shows the classification and describes the adverse effects of some CECs reported in the literature on living organisms, as demonstrated in experiments using different models, such as organism types, cells and/or organelles. In this way, it is possible to obtain data on the toxicity. This characteristic is related to the chemical structure of the CEC, its physicochemical characteristics, the environment in which it is found and the biological environment it has entered (Bila & Dezotti, 2007).

Groups	Contaminants	Origin	Spread	Effects	Reference
Perfluorinated Compounds (PFCs)	Perfluoro octane sulfonate (PFOS), perfluorooctanoic acid (PFOA) and their salts.	Firefighting foams, lubricants, metal spray coatings and detergents, paints, varnishes, coating formulations (for walls, furniture, carpets and food packaging), waxes, and water and oil repellents for leather, paper and textiles.	Direct and indirect sources, such as degradation of volatile and neutral PFC precursors, water, air and soil. They have been found in wildlife, drinking water, human serum and breast milk.	They are persistent, bioaccumulative, carcinogenic hormone disruptors in animals and promote reproductive dysfunction.	Hardell et al. (2014) Arvaniti & Stasinakis (2015)
Human and veterinary pharmaceuticals	Fluoxetine, α-ethinylestradiol (EE2), diclofenac, ibuprofen, sulfamethoxazole, paracetamol, ethinylestradiol, paraxanthine, atorvastatin, carbamazepine, estriol, venlafaxine, ranitidine, spiramycin, zidovudine and amoxicillin	More than three thousand different chemical products are used in human medicine, including lipid regulators, anti-inflammatories, analgesics, contraceptives, neuroactive drugs, antibiotics and beta-blockers. Veterinary products include antimicrobials, anthelmintics, steroids and non-steroids, anti-inflammatories, anti-parasitic, astringents, estrous synchronization, nutritional supplements and growth promoters.	Human excretion in municipal wastewater, hospitals, pharmaceutical waste, and landfills.	Ecotoxicological effects on non-target species. Increased antibiotic resistance in microorganisms, new strains of resistant bacteria, chronic toxic effects.	Smith et al., (2002) Thomas & Hilton (2004) FENT et al (2006)
Microplastics (MPs)	Bisphenol A (BPA), organophosphorus esters (OPEs), phthalic acid esters (PAEs), various types of phthalates.	Plastic packaging, degradable plastics, textile products, personal care products, paints and lubricants. The main polymers are nylon, acrylic, polyester, polyamide and vinyl acetate. In addition, there are plastic additives that are adsorbed onto the MPs.	Air, water and soil. Ingestion through breathing, contaminated water and food.	May cause chemical and physical effects. Endocrine disruptors and carcinogenic. They can cause respiratory and cardiovascular disease, and affect the digestive, respiratory, endocrine, reproductive, and immune systems. Transporters of other CECs and plastic additives.	Campanale et al (2020) Cimmino et al (2020) Lee et al (2023)

Table 1: Examples of some CECs and their features

3.2.3 CECs studied in this research: SMX

This research selected Sulfamethoxazole (SMX) due to the attention they have received in recent years and identification in surface and groundwaters worldwide. In addition, both compounds severely affect the environment. Detailed information on this compound can be seen in Table 2.

Name	CAS	Molecular formula	Molar mass (g/mol)	Water Solubility	Chemical Structure
Sulfamethoxazole (SMX)	723-46-6	$C_{10}H_{11}N_3O_3S$	253.28	610 mg/L	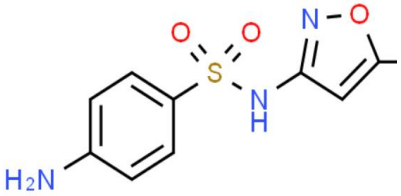

Table 2: Information on SMX (ChemSpider, 2024)

SMX is an antibiotic, bacteriostatic organic compound of the sulfonamide group, usually used with trimethoprim or cotrimoxazole. After ingestion, between 15% and 30% of orally ingested SMX is excreted in its original form (Mompelat et al., 2009), which is consistent with the United States Geological Survey (USGS) categorization, where SMX is among the 30 most commonly detected wastewater contaminants (Zhu et al., 2017). In this sense, it is considered persistent in the environment, as it has a half-life of 85 to 100 days, and its degradation in waterways takes about 52 days. In this way, during this time, SMX can contaminate the environment and living beings, interfering with embryonic growth, intoxicating microalgae by inducing the chloroplast translation mechanism, disrupting photosynthetic pathways and destroying cell wall synthesis, being catastrophic for the balance of trophic levels with a few μg/L, promoting bacterial resistance to the compound (Prasannamedha & Kumar, 2020).

3.3 Plastic solid waste (PSW)

3.3.1 Management of plastic solid wastes (PSWs)

The management process for plastic waste can be mechanical or chemical recycling, incineration for energy recovery, or landfilling. Accordingly, the American Society for Testing and Materials (ASTM) standard D5033-(2000) has defined four classifications of recycling (Al-Salem et al., 2009; Ragaert et al., 2017; F. Zhang et al., 2021):

- **ASTM I** - Primary Recycling: mechanical reprocessing of scrap materials with a controlled history to obtain products with properties similar to virgin plastics. Primary recycling, also known as closed-loop recycling, is applied to clean or semi-clean wastes and is particularly suitable for thermoplastics. This process is used in the same industry as scrap.
- **ASTM II** - Secondary Recycling: Mechanical reprocessing used materials into products with lower property requirements. It involves physical processes in the structure and is advantageous because it allows the plastic to be reused as a raw material in other plastic products.
- **ASTM III** - Tertiary Recycling: Recovery of valuable chemical components such as monomers or additives. Tertiary recycling involves the use of chemical processes to modify the structure of the plastic. Various chemical processes such as solvolysis, thermolysis, hydrolysis, glycolysis, aminolysis, gasification, hydrogenation, viscosity breaking, pyrolysis/thermal cracking, steam cracking or catalytic cracking are used in this process. PSW can also be used as a reducing agent in blast furnaces.
- **ASTM IV** - Quaternary Recycling: Energy Recovery. Quaternary recycling relies on the high calorific value of MSW to generate energy. This process involves incineration to produce steam, heat, and electricity. Various methods are used, such as single-stage direct combustion, fluidized bed, two-stage combustion, rotary kiln and cement kiln. However, there are atmospheric emissions associated with this approach.

These recycling processes can be illustrated in Figure 1. It is possible to understand that through tertiary chemical recycling using heat treatment, PSW can be transformed into monomers used in the polymerization of new plastic materials, preserving the physicochemical properties and value of the material (Jehanno et al., 2022).

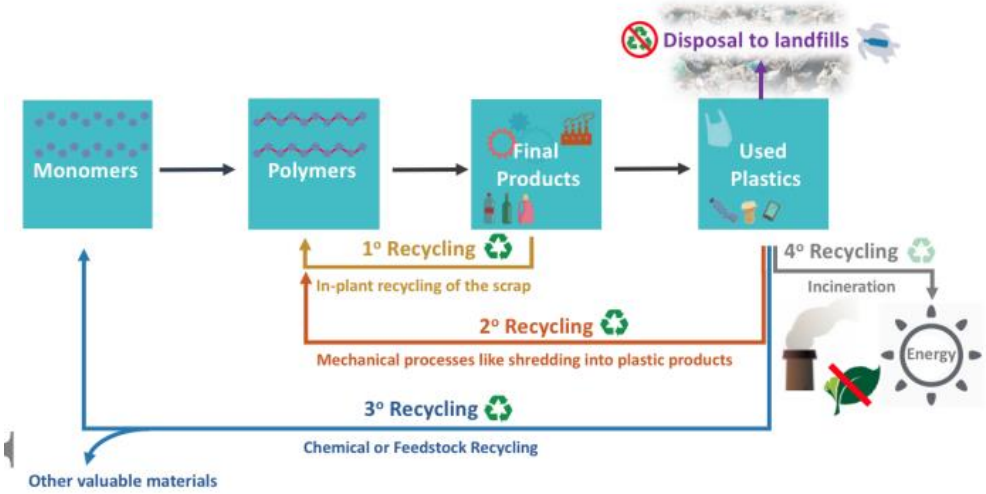

Figure 1. Types of recycling, adapted from Okan et al. (2018)

In these recycling processes, there are several challenges: to keep the final cost of the recycling process lower than that of synthesizing an equivalent virgin polymer from petroleum, to obtain a final plastic produced with recycled material with a quality superior or equal to its equivalent virgin, or even to incorporate the polymer obtained from PSW in high-tech materials. The most challenging approach to the recovery of PSW is called upcycling, which aims to use plastic waste as an abundant and inexpensive chemical feedstock for the synthesis of materials or molecules with higher final value. It still faces chemical, economic, and environmental issues that some studies are trying to overcome, for example, the inclusion of life cycle analysis of end-of-life plastic materials to guide the development of recycled plastic materials (Singh et al., 2022) and problems of waste collection and segregation to integrate it into a circular economy (Silva et al., 2022; Jehanno et al., 2022).

3.3.2 Recovery of plastic waste (RPW) and upcycling

Some alternatives have been explored for the recovery of plastic waste (RPW), such as the development of sustainable nanomaterials and nanocomposites from recycled plastics that can be used in a wide range of applications, replacing part of the conventional production of oil-based polymers, reducing the consumption of fossil fuels, the atmospheric emissions caused by this manufacturing process, the amount of PSW discarded into the environment, and increasing the insertion of plastic waste into a circular economy (Carroccio et al., 2022).

This process occurs in tertiary recycling through thermal treatment such as pyrolysis, gasification, and combustion. The pyrolysis is promising compared to other methods of PSW recovery, especially in terms of reduced environmental pollution and carbon footprint (Al-

Salem et al., 2017). Pyrolysis is a good option because it allows for producing monomers that can be used in various products. It also shows greater flexibility in using contaminated or mixed plastic waste, such as food packaging, mainly PE, compared to mechanical approaches to PSW recovery (Peng et al., 2022).

An example of the pyrolysis process is the recovery of PSW through the production of CNTs, which will be discussed in more detail in later topics of this thesis. The process of producing nanotubes can be carried out by heating and gasifying PSW in an inert atmosphere so that the monomers are transported by evaporation and deposited on a metal substrate, where the growth and formation of CNT structures occur (Sharma & Batra, 2020; Y. S. Zhang et al., 2021). In addition, in the last decade, the means to produce CNTs on a large scale have been researched and developed, providing an opportunity to evaluate different sources of recycled PSW and MSW to be used as raw materials in different CNT manufacturing processes (Bazargan & McKay, 2012; Diaz de Tuesta et al., 2023)

Another way to utilize PSW is to incorporate monomers from recyclable plastics into composite polymer membranes to upcycling this wastes. This topic will also be discussed in more detail in later sections of this thesis. These membranes can be made from a variety of polymers such as polyolefins (LDPE, HDPE and PP), polyamides, cellulose acetate, PET, polysulfones, among others, for the structuring and incorporation of nanomaterials and fibers (Lin et al., 2015; Ramírez-Martínez et al., 2023). The applications of these membranes are broad and can be used for water desalination, contaminant removal, fluid clarification, and solvent separation (Maiti & Pandey, 2022). These polymeric membranes can be a product to add value and promote the circular economy of PSW, also known as composite membranes, which can be produced by incorporating other compounds derived from the valorization of PSW, such as CNTs. In addition, many of these nanocomposites have been used in AOPs for water purification (Ribeiro et al., 2016; Li et al., 2023; Rawindran et al., 2024).

3.4 Advanced oxidation processes (AOPs)

Different types of AOPs exist, such as Fenton oxidation, ultrasonic oxidation, persulfate oxidation, photochemical oxidation, ozonation, gamma or electron beam irradiation, electrochemical oxidation, etc. Various factors influence these different types of AOPs, such as pH and the number of different ions: chloride ions, inorganic ions, phosphate ions, nitrate ions, etc (Saharan et al., 2014). There are specific applications, advantages, and disadvantages of each of these processes. The results of analyzing some of these processes are exposed in Table 3, which shows the main AOPs.

AOPs	Pollutants	Efficiency	Advantages	Disadvantages
Ozone oxidation	Active estrogenic compounds, manganese, iron and copper.	99%	Higher oxidation potential compared to chlorine Powerful oxidizer Ihibits bacteria and fungi Renewable source	High concentration required High process complexity
Electrochemical oxidation	Organophosphorus compounds and landfill leachate.	96%	Removes highly toxic compounds Does not generate hazardous by-products Does not require a catalyst	Energy source required Electrode maintenance Time-consuming
Fenton oxidation	Pesticides, phenols, formaldehyde, rubber chemicals and BTEX.	45–60%	Removes highly toxic compounds Does not generate dangerous by-products Does not require a catalyst	Produces ferrous waste Risk when storing and handling reagents
Photolysis and photocatalysis	Organic pollutants, Pharmaceutical compounds, pesticides, oil, textile dyes and grease	90–99%	Uses natural energy source Little catalyst used Minimal cost High physical stability	Low pH required Difficulty in isolating the catalyst Selective adsorption is low
Sonolysis	Persistent toxic compounds and organic solvent-water	71–82%	Does not use chemicals Removes medicines Short reaction time	Machines wear out Low efficiency High cost

Table 3: Features of the main AOPs (Saravanan et al., 2022)

Ozone oxidation uses ozone as a strong oxidant and follows the mechanism of adsorption and activation to produce reactive species. Electrochemical oxidation involves activation by electrocatalysts. Fenton-based oxidation consists of activating hydrogen peroxide by a catalyst containing iron and other metals such as cobalt, copper, manganese, and carbon-based materials, generating reactive species. In photocatalysis, the chemical reaction occurs through the compounds' absorption of ultraviolet, visible, or infrared light photons, generating free radicals. In sonolysis, ultrasound is used, and H_2O_2 may be added. Various catalysts are used to increase the production of radicals (Saravanan et al., 2022).

3.5 Catalytic wet peroxide oxidation (CWPO)

3.5.1 Fenton mechanisms

The catalytic wet peroxide oxidation (CWPO) or heterogeneous Fenton process, as described by Tyre et al. (1991), was developed to overcome the homogeneous Fenton reaction

(Fenton, 1894), by overcoming the disadvantages of high reactivity due to catalyst consumption and sludge generation due to the need to adjust the reaction pH. Today, CWPO is one of the most economically viable AOPs for the degradation of various CECs and water recovery for human consumption. This AOP is efficient at degrading recalcitrant organic compounds in industrial and municipal wastewater and has relatively low operating costs. In addition, the CWPO process can be used after conventional biological treatment for urban wastewater or before it for industrial wastewater, as CWPO can increase the biodegradability of recalcitrant compounds, thereby facilitating and increasing the efficiency of conventional biological treatment. The efficiency of CWPO depends on the catalyst, pH, temperature and concentration of hydrogen peroxide used in the process. Challenges that arise in CWPO include catalyst leaching and deactivation, more experimental studies with real wastewater matrices, studies in continuous fixed-bed reactors, and post-treatment toxicity (Rueda Márquez et al., 2018).

$$Fe\ (II) + H_2O_2 \rightarrow Fe\ (III) + {\cdot}OH + OH^- \quad (1)$$

$$Fe\ (III) + H_2O_2 \rightarrow Fe\ (II) + HO_2{\cdot} + H^+ \quad (2)$$

$$\text{Organic matter} + {\cdot}OH \rightarrow \text{Degradation products} \quad (3)$$

The complete mechanism of the Fenton reaction is still awaiting experimental validation, but according to what is currently known, hydrogen peroxide reacts with Fe (II) to produce -OH, and the main challenge of this process is the recovery of the catalyst due to the slow reduction kinetics of Fe(III) to Fe(II). In this sense, recent studies have shown that using electricity and light energy can accelerate the regeneration of Fe (II) in the Fenton reaction. Sunlight can be a cheap alternative to accelerate this process, as shown in Equation 4. In the presence of light (hv), pH 2.8, as can be seen from Equation 4, the $[Fe\ (OH)]^{2+}$ species, which are the key photoactive Fe (III) complex under sunlight, are reduced to Fe(II), generating even more -OH and increasing the rate of contaminant degradation, but creating the need to correct the pH before and after this process. In addition, a further challenge arises when the pH of the solution is raised to neutral, leading to the precipitation of iron sludge in the form of iron hydroxides (N. Thomas et al., 2021).

$$[Fe(OH)]^{2+} + hv \rightarrow Fe(II) + {\bullet}OH \quad (4)$$

These challenges give rise to the heterogeneous Fenton reaction, which can be carried out around neutral pH, and this process also uses iron-based catalysts with low cost, negligible toxicity, high catalytic activity and easy recovery methods. This heterogeneous Fenton system can take place via two routes (Nidheesh, 2015). One of the mechanisms describing these routes, which is widely accepted, was published by Lin & Gurol (1998), who proposed the

heterogeneous catalytic decomposition reactions of hydrogen peroxide using solid iron oxide (goethite), which is the heterogeneous catalyst due to the recycling of Fe(III) and Fe(II) on its surface, In this process, the hydroperoxyl radical (Fe II + HO_2-) is formed via a complex which, together with H_2O_2, leads to the formation of Fe III-OH and -OH, which will decompose the micropollutants. In addition, in this process, the second pathway occurs via the iron leached from the catalyst, which provides the homogeneous Fenton catalysis reaction, increasing the reaction rate.

3.5.2 Catalysts for CWPO

Among the most widely used catalysts are iron oxides, which are considered to be biodegradable, non-toxic, environmentally friendly and have a low leaching rate. The physical properties of these catalysts are related to the method of synthesis, which determines the specific surface area, morphology, and particle size. These materials also can act as photocatalysts. Some of the mineral classes used as Fenton catalysts are hematite, magnetite, ferrihydrite, goethite, ferrihydrite, schwertmannite and lepidocrocite. Composite materials of iron oxides doped with transition metals, called ferrites, are the most widely used due to their easy separation and reuse, magnetic properties and general formula $M_xFe_{3-x}O_4$ (M is a divalent transition metal ion) (Rahim Pouran et al., 2014).

Other metals can be used as catalysts in CWPO, and metal substrates supported on different non-metallic materials such as carbonaceous (de Freitas Batista et al., 2022), clay (Santos Silva et al., 2019), graphene oxide (GO) (Cruz-Alcalde et al., 2022), activated carbon (AC) (Diaz De Tuesta et al., 2021), hydrochar (Roman et al., 2021), CNTs (Roman, Diaz de Tuesta, et al., 2023), multi-core (A. S. Silva et al., 2023). These materials increase the rate of catalytic degradation of contaminants because they provide high surface area, good mechanical stability, and better electron transfer (N. Thomas et al., 2021).

3.6 Catalytic nanocomposite membranes (CNMs)

3.6.1 Materials and manufacturing process

CNMS are membranes composed of catalytic nanoparticles. The choice of materials is important and must take into account the objectives and parameters of the membrane application. Inorganic membranes (oxides, ceramics and metals) can be used as a base. They have greater thermal, chemical and mechanical resistance, but have the disadvantage of being more economically expensive and some of them have low hydrothermal stability. Polymeric membranes (PMs), on the other hand, are less expensive, more sustainable, allow better quality

control, are easier to produce and in larger quantities, but have the disadvantage of being less durable and having a shorter life. Another manufacturing factor is the wide variety of nanocomposites that can be incorporated into CNMs: 2D nanomaterials, CNTs with metal substrates, covalent metal-organic frameworks (MOFs/COFs), metal oxides, metal sulfides and their composites, other catalytic materials without metallic elements such as graphene, graphitic carbon nitride (gC3N4), CNTs, carbon quantum dots (CQDs), etc. (Yin & Deng, 2015; Chen et al., 2023).

The manufacture of CNMs also depends on the choice of polymer matrix. The most used polymers are polyvinylidene fluoride (PVDF), polysulfone (PSF), and polyethersulfone (PES). Due to the excellent chemical and physical stability of these polymers and their superior thermal and mechanical properties, as shown in Table 4, membranes are also produced with (PVC), polypropylene (PP), polyacrylonitrile (PAN), and cellulose acetate (CA) (Ahmad et al., 2013). Polyvinylpyrrolidone (PVP) and polyethylene glycol (PEG) have been widely used as additives in the preparation of these membranes to increase their hydrophobicity (Marbelia et al., 2019). PVP also helps to form larger pores during the phase inversion fabrication process and improves the viscosity of the forming solution (Kourde-Hanafi et al., 2017).

Polymer	Advantages	Disadvantages	References
PES	It has thermal, chemical and physical resistance over a wide pH range (1 to 13) and is also easy to process.	Susceptible to fouling and can cause a low flux in the membrane	Shen et al. (2012)
PSF	It has thermal, chemical and physical stability, greater resistance to oxidation by chlorine.	Can be fouled by molecules smaller than its pores	Saljoughi & Mousavi (2012)
PVDF	It has thermal stability, resistance to radiation and a wide pH range, high organic selectivity.	Can be fouled by organic contaminants and suffers from reduced flux	Yuliwati & Ismail (2011)

Table 4: Main polymeric materials used in the manufacture of CNM.

The choice of materials for the fabrication of CNMs depends on the compatibility between the polymer substrate and the nanocomposites, as well as the purpose of the application, since they define the membrane properties, permeability, selectivity, and its efficiency. There are a variety of specific methods for preparing CNMs, including phase inversion, sintering, stretching, electrification and track etching, dip coating and template leaching, colloidal precipitation method, interfacial polymerization, etc. However, the fabrication techniques can be generalized into three main groups: mixing methods, in situ growth, and surface deposition, as shown in Table 5, which lists the advantages and

disadvantages of these methods. In view of this, the most widely used and commercialized method today is the phase inversion technique, which processes the polymer from a liquid phase to a solid phase, after the mixing method, within this technique there are still other methods: non-solvent induced phase separation (NIPS), thermally induced phase separation (TIPS), vapor induced phase separation (VIPS), evaporation induced phase separation (EIPS) and colloidal precipitation (Rajlaxmi et al., 2021; Chen et al., 2022).

Method	Process	Advantages	Disadvantages	References
Mixing method	Forming processes such as film coating, tape casting or dip coating, dry/wet phase inversion. The catalyst is introduced into the polymer matrix in a suitable solvent or solution and uniform dispersion is achieved by stirring or ultrasonic treatment. The catalyst is then solidified into a membranous structure.	Easy operation, excellent processability, control and greater stability	Time-consuming and requires more chemicals	L. P. Zhang et al. (2020)
In situ growth	Processes similar to conventional supported catalyst preparation methods, including impregnation, adsorption and precipitation of the final catalysts. The membrane substrate is immersed in the catalyst precursor solution, after a period of complete adsorption, the catalyst is generated in situ on the surface or inside the membrane by post-treatment operations such as reduction, activation and drying.	Excellent stability, highly exposed catalysts and effortless control	Non-uniform deposition, strict reaction conditions, slow, difficult to replicate on a large scale	Zhao et al. (2020)
Surface deposition	Direct catalyst deposition processes on the membrane surface. The catalyst is physically or chemically adsorbed to the substrate surface using ion-assisted deposition (IAD), CVD, atomic layer deposition (ALD) or vacuum filtration.	Simple, economical, adaptable operation, fast manufacturing and effortless control.	Presence of impurities or defects and unstable deposition.	De Filpo et al. (2018)

Table 5: Main methods of manufacturing CNMs, Chen et al., 2023

The non-solvent induced phase reversal (NIPS) method is the most widely used and will be investigated in this research project. To perform this method, it is important to choose the correct solvent and concentration of the polymer solution. This solution is then formed on a flat surface and immersed in a bath containing a non-solvent (coagulant), such as water. During this process, there is an exchange between the solvent and the non-solvent, resulting in phase separation and the formation of the membrane. The structure of the membrane can be adjusted by controlling factors such as the concentration of the polymer solution, the non-solvent used, the temperature of the bath, or the evaporation time. In general, this method is used to create asymmetric membranes with a porous layer at the bottom and a dense layer at the surface (Aburabie et al., 2017).

3.6.2 Properties of CNMs

The characteristics of an efficient membrane include certain technical requirements, such as maintaining a high filtration flux, low filtration pressure, compactness to save space and reduce manufacturing costs, durability and efficiency to prevent fouling. The operating parameters for membrane separation are pressure, concentration gradient and hydrostatic pressure, which allows ultrafiltration. The main characteristics of membranes are selectivity and membrane permeability. Permeability (J) [L m^{-2} h^{-1}], indicates the mass transfer capacity of the membrane, which is the permeate mass flow rate across the membrane (V), per unit area (A) [m²] and time (Δt) [h]. A high permeability value can indicate high process efficiency, J is also related to the selectivity (α), which is inversely proportional because α is the ratio between the input flux ($F1$) and the output flux ($F2$) permeated by the membrane (Ng et al., 2013; Lu et al., 2021).

$$J = \frac{V}{A\Delta t} \quad (5)$$

$$\alpha = \frac{F2}{F1} \quad (6)$$

Synergistic effects between membrane components modify these properties in CNMs. An example of this is the regulation of the membrane structure, where the permeability is modified by adding some type of catalyst to its polymeric matrix. This property is proportionally related to the pore size and hydrophilicity of the PMs. Since the most widely used membranes today tend to be hydrophobic, being generally made of polyvinylidene fluoride (PVDF), polypropylene (PP) or polytetrafluoroethylene (PTFE), by adding some catalysts to a certain extent these membranes tend to have a more hydrophilic character, this characteristic can be quantified by measuring the water contact angle (WCA), i.e. they significantly improve their permeability. On the other hand, the amount of catalysts inserted in the membrane should be increased with caution, as the addition tends to reduce the pores of the membranes, so it must be proportional to the gain from the improvement in hydrophilicity or catalytic oxidation (Yang et al., 2019; L. Zhang et al., 2021).

The stable and dispersed storage of the catalysts are some of the advantages of using these composites, this system is made by a two-dimensional/three-dimensional membrane that stores and disperses the catalyst, this allows the catalytic reactions to take place on the surface of the membranes or in their pores, instead of inside a feed solution, it also prevents the uneven dispersion and agglomeration of powdered catalysts in conventional catalytic processes, especially with CNT suspensions, which reduces the use of these materials (C. Chen et al., 2022). In addition, this stable storage avoids the loss of catalysts in continuous processes and

allows better recycling of this material in membranes, although it is still necessary to evaluate the leaching rate at the end of catalysis, although some studies show low values for some metal substrates immobilized in CNMs (Molnár & Papp, 2017).

The nanoconfinement effect is also an advantage of combining catalysts with CNMs. This phenomenon occurs in the pores of membranes that act as micro or nanoreactors, and these confined catalytic reactions have provided a new way to utilize CNMs. The pores of these membranes allow the pollutants to be rapidly introduced along with the oxidants to immediately release the radicals that degrade the organic pollutants, avoiding the loss of these degradants due to their short lifetimes, an example of which are reactive oxygen species (ROS) such as -OH and -OOH. In this way, there is an increase in the availability of free radicals, an increase in the mass transfer of these formed radicals to the CECs in the aqueous phase, accelerating the catalytic process through the nanoconfinement effect (S. Zhang et al., 2021; (Ly et al., 2023).

The efficient removal of natural organic matter (NOM) from AOPs is also one of the advantages of using CNMs. NOM is known to be present in surface water and effluents and to act with competitive adsorption and ROS scavenging capacity, which can block the catalytic site, quench hydroxyl and peroxyl radicals, inactivate the heterogeneous catalyst, reduce catalytic efficiency and generate harmful by-products. In this way, CNMs can prevent organic macromolecules larger than their pores from interfering with the catalytic process and allow micropollutants to permeate (Lindsey & Tarr, 2000; J. Lu et al., 2016; Xie et al., 2021).

3.6.3 CNMs with CNTs

The first polymer nanocomposites (NP) using carbon nanotubes as filler were reported by Ajayan et al. (1994), the concept of PMs formed by CNTs emerged with Sun & Crooks (2000). Since then, CNTs have been widely explored in the preparation of polymer nanocomposites membranes (PNMs) by various synthesis methods, material combinations, and methods for decomposition of organic pollutants in AOPs as CNMs, these forms membranes called CNMs based on CNT, and other applications such as water desalination, removal of heavy metal ions, and oil-water separation. The incorporation of CNTs can help with the problems of compensation between permeability and selectivity of CNMs, as well as increase physicochemical resistance and reduce surface fouling (Barrejón & Prato, 2022).

For example, SWCNTs provide larger pores and more voids in the membranes, increasing their porosity and permeability. They also impart a less hydrophobic character to the membranes compared to MWCNTs of the same diameter. In addition, small-diameter

SWCTs allow the fabrication of vertically aligned CNT platforms that form membranes with high density, permeability, and selectivity that exceed those of conventional nanofiltration and ultrafiltration membranes. Despite the hydrophobic nature of CNTs, the water flux in the membrane tends to increase with increasing nanotube layers (Rizzuto et al., 2018).

The fouling of the membranes decreases when CNTs are inserted, an example of which is the self-cleaning effects, where catalysts are added to the surface pores to promote water oxidation and generate oxygen from polyoxometalates, creating oxygen bubbles in the presence of hydrogen peroxide that remove the fouling material from the surface (Toma et al., 2010; Bonchio et al., 2019).

The addition of functionalized CNTs to the membranes shows increased hydrophilicity, forming negatively charged membranes, due to the insertion of functional groups on the surface of the CNTs that result in changes in porosity, surface roughness, compensation between permeability and selectivity, also reduces surface fouling, since the foulants are generally negatively charged hydrophobic. In addition, by converting non-polar hydrophobic CNTs into polar hydrophilic CNTs, the addition of certain chemical groups increases the interaction between CNTs and polymers. This in turn leads to an increase in the porosity of the membrane, which strongly affects the rheological properties of the final membrane (Rana & Matsuura, 2010; F. Xu et al., 2019).

There are three different types of carbon nanotube membranes, vertically aligned CNTs (VA-CNTs), composite membranes based on dispersed CNTs (CCPS-CNTs) and buckypaper CNTs (BP-CNTs). VA-CNTs are made of nanotubes that form a vertical distribution, have a high density, the manufacturing process is complex, can be done by CVD and subsequent oxidation attack to open the ends of the CNTs, these form highly efficient channels for rapid passage of fluid, but have lower mechanical resistance than the other types. BP-CNTs are membranes formed by a 3D network of randomly arranged CNTs held together by van der Waals force and π-π interactions between them, it has high porosity and specific surface area, the manufacturing method is simple, involves purification, dispersion in solvent, mechanical or ultrasonic agitation, vacuum filtration and drying, has moderate water flow rate, but also has limited mechanical strength compared to CPS-CNTs. (Ali et al., 2019; Khan et al., 2021; Barrejón & Prato, 2022).

CNT-CPs membranes are formed by heterogeneous structures of CNTs randomly dispersed on the surface or in the inner layer of a polymer matrix. Due to their properties such as high flexibility, π-π interaction with aromatic compounds and low internal friction coefficient, they can improve some properties of CNMs: increased operational stability of the

membrane, which occurs due to interfacial adhesion between the substrate, CNTs and polymer. Improved mechanical strength due to the strong C-C bonds of the graphitic layers (Wu et al., 2016). Improved permeability due to the dispersion of CNTs in the polymer matrix, which provides greater porosity (Sianipar et al., 2017). Porosity can be defined according to the type and diameter of the CNTs inserted, facilitating the retention of ions and organic molecules (Ismail et al., 2009). Furthermore, although CNTs increase the hydrophobicity of the membrane, the increase in permeability is even more rewarding, as shown by the results obtained by Tijing et al. (2016).When incorporating 5% CNTs in a PVDF membrane, they obtained an increase in hydrophobicity, reaching superhydrophobicity. This was tested by analyzing the contact angle measured at 158.5º, however, they obtained an increase in saltwater permeability of up to 59%, which could be due to the slippery properties of the CNT layers (Barrejón & Prato, 2022).

As CNTs are hydrophobic, this can lead to some challenges in the production and use of membranes: the nanotubes may not be homogeneously dispersed in the solvent, there may be adsorption problems and adverse reactions. Air oxidation or acid oxidation is one of the most widely used methods to introduce functional groups such as -CO, -COOH and -OH into the walls of CNTs, increasing their hydrophilicity, stability, solubility in organic solvents, dispersion and affinity with the polymer matrix, as well as increasing pores and roughness, which increases the permeability of the membrane; on the other hand, decreasing hydrophobicity reduces the adsorption of non-polar organic compounds (Sianipar et al., 2017; Ihsanullah, 2019).

3.7 CWPO intensified filtration using CNMs

Some authors have obtained promising results by using CNMs based in CNTs to degrade CECs in AOPs, as can be seen in Table 6. However, there are few studies that explore this combination with CWPO, consulting the Scopus and Web Of Science (WoS) databases, searching for "carbon AND nanotube AND membrane AND peroxide AND smx OR Sulfamethoxazole" for article title, abstract, keywords via Scopus and All Fields on WoS, for each year from the beginning, it was possible to find only 1 publications of these categories applied to remove SMX by Xia et al. (2023).

As an example of the low number of studies in this area, a search for general words on this subject, replacing "peroxide" with "oxidation", increased the results and it was possible to find 15 studies via WoS and 11 via Scopus, removing repeated studies only 12 of these use some CNMs in some AOPs, with peroxydisulfate (PDS), peroxymonosulfate (PMS) or H_2O_2

activation, most of the other studies found are CNMs applied in electrochemical oxidation.. The main studies most like this work are shown in Table 6.

No publication was found on the specific incorporation of CNTs fabricated on a IO/Al_2O_3 in CNM (PVP/PVDF) to degrade SMX in a continuous CWPO system. An attempt was made to replace the term "peroxide" with "oxidation", but no results were obtained with similar work. In view of these searches, it is possible to see the recent application of CNMs in the last 4 years. the largest used peroxymonosulfate (PMS) activation. On the other hand, Xia et al. (2023) comparatively tested PMS, PDS and H_2O_2, and the results showed that PMS has a higher yield in the decomposition of SMX. In addition, evaluating the experimental parameters of these studies, it is noteworthy that there is a lack of tests with real or similar matrices, as well as the range of concentration of the pollutant used in the system, from 500 μg/L to 30 mg/L, which is related to the wide variation in the concentration of oxidants, was described by Ribeiro et al. (2022) as a difficulty in comparing results and membrane efficiency.

Author	Title	Catalytic membrane	AOP nethod and characteristics	Pollutant and concentration	Water matrix	Pollutant removal
Ma et al. (2024)	New insights into Co_3O_4-carbon nanotube membrane for enhanced water purification: Regulated peroxymonosulfate activation mechanism via nanoconfinement	Co_3O_4-in-CNT membrane showed a superfast SMX removal. Demonstrated nonradical-to-radical mechanism transformation were ascribed to the nanoconfinement effect in CNT	Peroxymonosulfate (PMS) [0.33 mM]	Sulfamethoxazole (SMX) [0.04 mM]	Deionized water	99.5% SMX after <1 min
Xia et al. (2023)	Effects of peroxide types on the removal performance and mechanism of sulfonamide antibiotics using graphene-based catalytic membranes	rGO/N-CNT membranes of reduced graphene oxide and nitrogen-doped CNTs were loaded at a dosage of 8 g/m² onto a nylon membrane	Peroxydisulfate (PDS) Peroxymonosulfate (PMS) Hydrogen peroxide (H_2O_2) All: [1 mM]	Sulfamethoxazole (SMX) Sulfadiazina (SDZ) Sulfamerazina (SMR) Sulfametazina (SM2) All: [500 μg/L]	Deionized water Surface water	93% SMX 98% SDZ 99% SMR 90% SM2 After 10h
Qian et al. (2022)	Carbonaceous composite membranes for peroxydisulfate activation to remove sulfamethoxazole in a real water matrix	Membrane composed of NG/rGO/CNTs.Mixture of N-doped graphene, reduced graphene oxide, and carbon nanotubes (vacuum filtration).	Peroxydisulfate (PDS) [2 mM]	Sulfamethoxazole (SMX) [500 μg/L]	Deionized water Tap water Surface water Effluent from aerobic tank Effluent from anoxic tank	23.03 mg/m²h 22.15 mg/m²h 7.32 mg/m²h 10.84 mg/m²h 3.95 mg/m²h After 24h
Ye, Dai, Li, et al. (2021)	Lawn-like Co_3O_4@N-doped carbon-based catalytic self-cleaning membrane with peroxymonosulfate activation: A highly efficient singlet oxygen dominated process for sulfamethoxazole degradation	Co_3O_4@NCNTs/g-CN membrane made of nitrogen-doped carbon nanotubes with Co3O4, grown in-situ on gC_3N_4. CoxOy@CCNM achieved instantaneous antibiotic degradation efficiency under flow filtration	Peroxymonosulfate (PMS) [0.2 g/L]	Sulfamethoxazole (SMX) [10 mg/L]]	Deionized water	98.9% SMX after 20min

Table 6: CNMs studies applied to AOPs of SMX

4 MATERIAL AND METHODS

4.1 Reactants

4.1.1 CNTs synthesis

- Iron (II) chloride tetrahydrate (98%), Across Organics.
- Iron (III) chloride hexahydrate (97%), VWR Chemicals.
- Absolute ethanol (99.8%), Fisher Chemical.
- Ethylene glycol (99%), Fisher Chemical.
- Alumina, BASF in pellets form.
- Low-density polyethylene (LDPE), average Mw ~ 35,000 g mol^{-1}, Sigma-Aldrich.
- Sulfuric acid (95%), VWR Chemicals.

4.1.2 CNMs synthesis

- Polyvinylpyrrolidone (PVP; MW: 40,000 g mol^{-1}), Sigma Aldrich.
- 1-methyl-2-pyrrolidone (NMP; 99.5 wt%), Sigma Aldrich.
- Poly(vinylidene fluoride) (PVDF; MW: 275,000 g mol^{-1}), Sigma Aldrich.

4.1.3 SMX filtration enhanced by CWPO

- Sulfmethoxazole (98%), Alfa Aesar.
- Hydrogen peroxide (30%), VWR Chemicals.

4.1.4 Analytical measurements

- Orthophosphoric acid (85%).
- Sodium sulphite anhydrous (98%).
- Titanium (IV) oxysulfate (99.99 *wt.*% metal basis, *c.a.* 15 *wt.*% solution in dilute sulfuric acid).
- All chemicals were used as received.
- Ultrapure and distilled water have been used for solution preparation and washing procedures during this work.

4.2 Synthesis of CNTs

The CNTs were prepared according to previous works (Diaz de Tuesta et al., 2023). The nanomaterials were synthesized by CCVD using iron oxide supported on alumina as a metal substrate. The metal substrate was prepared by sol-gel method (A. S. Silva et al., 2023). In brief, two separate solutions were prepared: one comprising 20 mL of ethanol containing 10 mmol of $FeCl_2 \cdot 4\ H_2O$, and the other consisting of 80 mL of ethylene glycol with 20 mmol of $FeCl_3 \cdot 6\ H_2O$. Each solution was individually stirred and heated, with the former at 80 °C and the latter at 60 ºC, before being cooled to room temperature. Subsequently, both solutions were combined with 6.6 g of alumina and thoroughly mixed. The resulting mixture underwent heating at 60 °C for 2 hours, followed by further heating until reaching 120 °C, resulting in a gel-like consistency, and finally heated to 210 °C until a dry powder was obtained. The synthesized powder underwent calcination initially at 300 °C for 12 hours and then at 600 °C for 24 hours in an air atmosphere, yielding iron oxide supported on alumina, denoted as IO/Al_2O_3 catalyst.

The CVD process was carried out in a one-chamber reactor shown in Figure 2. The reactor is equipped with three independent heating zones and 2 crucibles. In this process, the LDPE located at the top of the reactor is vaporized and transferred to the particles of the magnetic iron oxide and alumina catalyst (IO/Al_2O_3) located at the bottom of the reactor. For each batch of the process, 5 g of LDPE is added to the upper crucible and 1 g of IO/Al_2O_3 catalyst is added to the lower crucible. The furnace is then heated to 850ºC in the upper zone and 450ºC in the lower zone and maintained in an inert nitrogen atmosphere at a constant flow of 80 mL min^{-1} for 1.5 hours. Finally, the N_2 gas flow is maintained until the furnace cools to room temperature. LDPE, a carbon-rich polyolefin, is used because it is an abundant plastic material and grows on the catalyst to form CNT structures called $CNT@IO/Al_2O_3$.

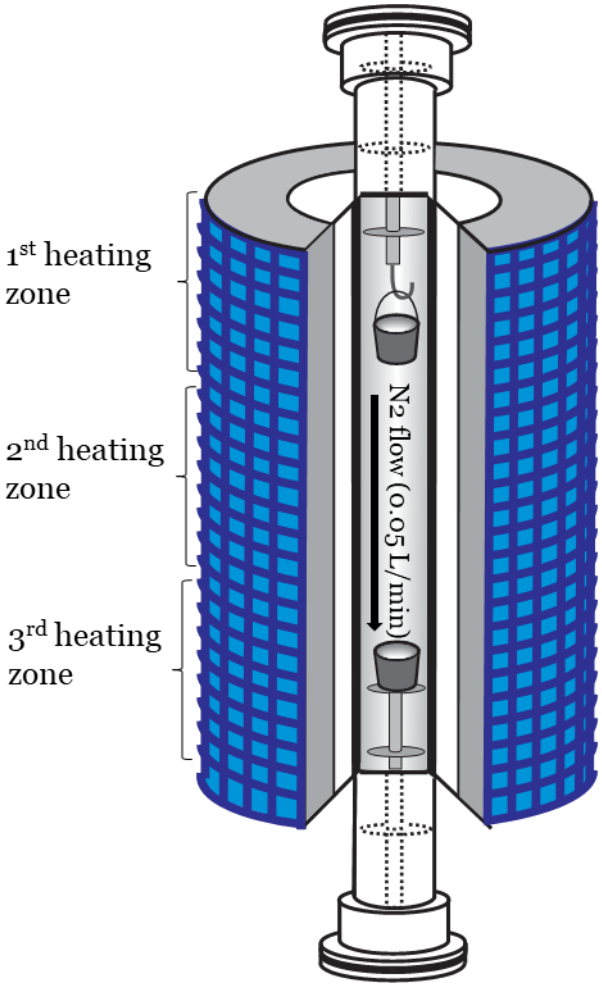

Figure 2. Catalytic chemical vapor deposition (CCVD) reactor used to synthesize carbon nanotubes (CNTs).

4.1 Synthesis of acid-washed CNTs

The CNTs material obtained is purified in acid to remove the remains of the magnetic catalyst and any radicals that may have formed in the CNT structures, such as amorphous carbons (Diaz de Tuesta et al., 2023). In this way, this material is added to sulfuric acid H_2SO_4 (50%) in a ratio of 50mL per 1g in a flask heated to 170º for 3 hours. The material is then vacuum filtered with 0.45 µm nylon filters and washed successively with distilled water until rinsing waters reach neutral pH, as shown in Figure 2. Finally, the washed CNTs are dried in an oven at 60ºC for 12 hours. They are then named CNTW@IO/Al_2O_3.

Figure 3. System for acid washing CNTs

4.2 Synthesis of CNMs

The composite membranes were prepared according to the adapted procedure published by the group (Ribeiro et al., 2022) by mixing reagents and phase inversion. For this purpose, 0.070 g of polyvinylpyrrolidone (PVP) which imparts a hydrophilic character to the membranes, was dissolved in 6 mL of 1-methyl-2-pyrrolidone (NMP) to which 0.234 g of CNT @IO/Al_2O_3 or CNTW@IO/Al_2O_3 was added, corresponding to 3.2 wt% of the membrane-forming materials, Figure 4a. The solution was then kept in the ultrasonicator at room temperature for 3 hours, Figure 4b. Then 1.07 g of poly(vinylidene fluoride) (PVDF) was added to give strength and hydrophobicity to the membranes. To start the polymerization, this solution was stirred (150rpm) and heated at 40 ºC for 48 hours, at the end of this stage, Figure 4c, the solution was left at room temperature and without stirring for about 12 hours, the result was a viscous solution that was stretched to a thickness of 100 µm on a glass plate in the casting knife film applicator (Elcometer 3580, Warren) Figure 4d.

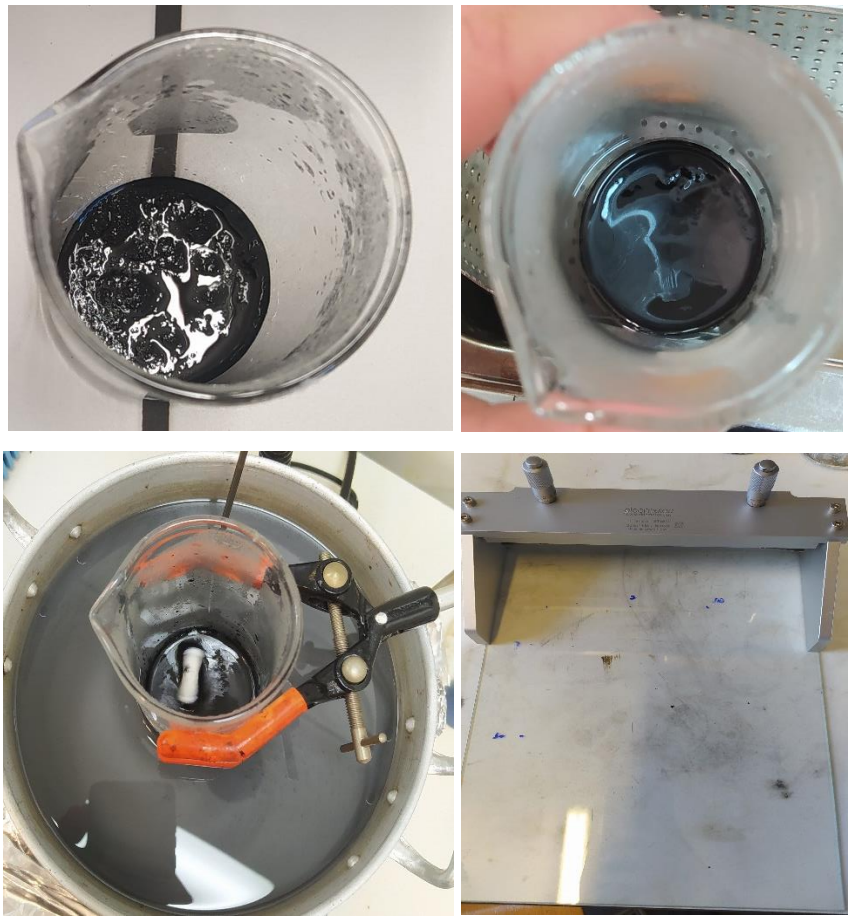

Figure 4. (a) Mixture of PVP, CNT and NMP (b) Homogenized solution of PVP, CNT and NMP (c) Solution with added PVDF stirred in an oil bath (d) Casting knife film

N-Methyl-2-pyrrolidone (NMP) was chosen as the solvent due to its ability to dissolve the PVDF polymer at a relatively low temperature, which is advantageous for membrane fabrication. Additionally, NMP has proven to be more effective in dispersing CNTs, both functionalized and pristine, compared to other solvents like N,N-dimethylformamide (DMF). This improved dispersion of CNTs is crucial for ensuring a homogeneous distribution of the nanocomposites within the polymer matrix. Another important factor in choosing NMP was its relatively lower toxicity compared to DMF, making the process safer and more environmentally friendly (T. L. S. Silva et al., 2015a).

The stretched solution was immersed in water for coagulation and then stored in containers with distilled water. This resulted in the formation of the composite membrane Figure 5a. On the day of the filtration tests, they were cut into pieces with an internal diameter of 1.64 cm and an effective area of 2.10 cm^2 to fit the diameter of the membrane reactor, as can be seen in Figure 5b and the parts of the membrane reactor (Figure 6).

Figure 5. (a) PVP/PVDF@CNTW membrane after molding and coagulation (b) Cut PVP/PVDF@CNTW membrane.

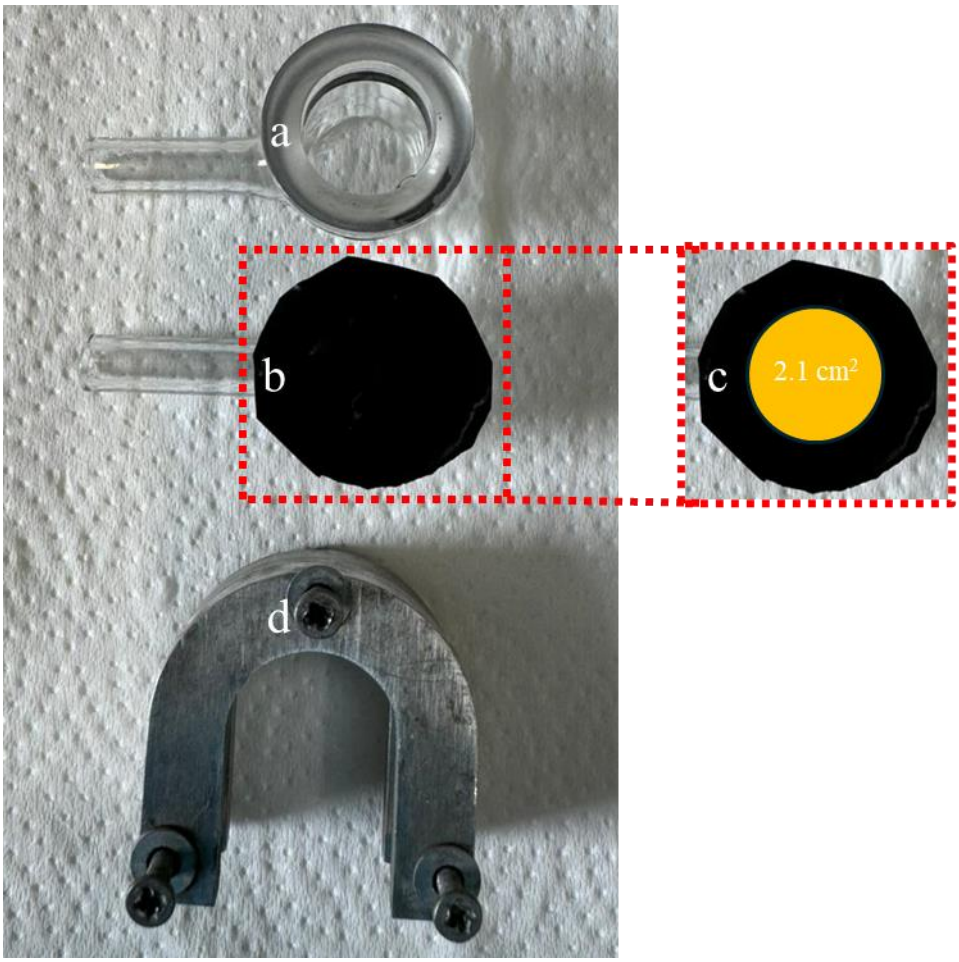

Figure 6. (a) Upper part of the membrane reactor, (b) lower part loaded with polymeric composite membrane, (c) representation of the membrane effective area, and (d) metal support that holds the reactor together.

In addition, other membranes were produced to critically compare their performance in removing the pollutant and test the intensification of filtration; the 4 membranes produced are described in Table 7. below.

Membranes	Production features
PVP/PVDF@CNT	Membrane produced with CNT@ IO/Al_2O_3 without chemical treatment.
PVP/PVDF@CNTW	Membrane produced with CNTW@IO/Al_2O_3 that have been synthesized and acid-washed with sulphuric acid.
PVP/PVDF@IO/Al_2O_3	Membranes made only with 0,09g of metal substrate IO/Al_2O_3 (catalyst) in the same quantity present in 0,234g of CNTs in this study.
PVP/PVDF	Polymeric membrane made only with the base polymers PVP, NMP and PVDF.

Table 7 Membranes produced.

4.3 Characterization of the materials

4.3.1 Textural properties

The textural properties of the composite membranes were thoroughly investigated through nitrogen (N_2) adsorption-desorption isotherms measured at 77 K, using a Quantachrome NOVATOUCH LX4 adsorption analyzer. This technique provides critical insights into the surface area, pore volume, and porosity of the membranes by evaluating the gas-solid interactions under controlled conditions. Adsorption-desorption isotherms are generated by monitoring the amount of nitrogen gas adsorbed on the membrane surface at various relative pressures (p/p0), where p0 is the saturation pressure of nitrogen at 77 K. The specific temperature and pressure conditions are crucial to ensure nitrogen condensation in the porous structures, allowing for a detailed understanding of the microstructural features of the materials.The BET model assumes that gas molecules adsorb onto the surface in multilayers and is applied in the relative pressure range of p/p0 = 0.05 to 0.35, which corresponds to the optimal linear region for BET calculations. This range is critical to avoid errors that could arise from condensation in larger pores (capillary condensation) or from incomplete monolayer formation. The apparent surface area (S_{BET}), expressed in m^2/g. (Santos Silva et al., 2019)

Additionally, the total pore volume (V_T) was calculated based on the volume of nitrogen adsorbed at a relative pressure close to saturation (p/p0 = 0.98). At this pressure, the largest pores within the mesopore range (2-50 nm) are completely filled with nitrogen gas, enabling the calculation of both mesopores and micropores (<2 nm) using the Gurvitch rule. This rule

is particularly useful for estimating the cumulative pore volume, as it assumes that at this relative pressure, the adsorbed nitrogen behaves similarly to a liquid phase, facilitating the differentiation between micropores, mesopores, and macropores. This cumulative volume is critical for understanding the material's ability to adsorb and transport fluids or gases, which is fundamental in assessing membrane performance in separation and filtration applications. By combining BET surface area measurements with total pore volume analysis, it is possible to estimate the pore size distribution of the membranes, offering deeper insights into the structural properties that affect the membrane's efficiency in both filtration and catalytic processes (Rouquerol et al., 1999) .

4.3.2 Overall membrane porosity

The dry weight of the membranes was recorded, and they were immersed in isopropyl alcohol (IPA) overnight so the solvent could penetrate the membrane pores. After this process, the membrane weight was recorded and registered. The porosity was calculated according to Equation 7.

$$\varepsilon = \frac{(m_w - m_d)/\rho_{IPA}}{\frac{m_d}{\rho_d} + \frac{m_w - m_d}{\rho_{IPA}}} \cdot 100 \quad (7)$$

in which m_w and m_d represents the weight of the membranes wet and dry, respectively, and ρ_{IPA} and ρ_P are IPA (0.786 g cm^{-3}) and polymer (1.78 g cm^{-3}) densities. The experiment was carried out in triplicate for each composite membrane and fallowing the adapted procedure in literature (Smolders & Franken, 1989).

4.3.3 Largest pore size

The bubble point method was adapted from the literature (T. L. S. Silva et al., 2015a), used to measure the largest pore size of the composite membranes. In brief, the membrane is saturated with IPA following the same procedure used to determine porosity. The membrane is then fixated in the reaction apparatus, and the pressure is slowly increased on one side using an inert gas (nitrogen). At a certain point, the liquid starts to leave the membrane pores, and gas bubbles can be observed on the opposite side of the membrane. The gas pressure required to start this phenomenon is known as bubble point. From this experiment, the largest pore diameter can be calculated according to Equation 8,

$$d_{pore} = \frac{4 \cdot \gamma \cdot cos\theta}{P_{bubble}} \quad (8)$$

In which γ is the surface tension of the liquid (2.17 mN m^{-1} for IPA), θ is the contact angle between the liquid and pore wall, and P_{bubble} (bar) represents the bubble pressure. The experiment was carried out with three membranes to determine the average pore diameter.

4.3.4 Hydrophilicity and Hydrophobicity

The hydrophilicity/hydrophobicity characteristic was measured by water contact angle measurements by the sessile-drop methodology using an Attention (model theta) optical tensiometer for image acquisition, adapting a methodology described elsewhere (Vieira et al., 2020). A water droplet (approximately 5 µL) was placed at the center of each membrane, and images were captured immediately using a high-resolution camera. These images were processed using ImageJ software to calculate the contact angle. The average contact angle was obtained by analyzing three droplets at different positions on the membrane surface to ensure measurement consistency. Wettability is a crucial parameter for membranes, influencing their interaction with liquids, permeability, and fouling behavior. In general, a low contact angle (below 90°) indicates a hydrophilic surface, which enhances water affinity and wettability, promoting better filtration performance in aqueous systems. On the other hand, a high contact angle (above 90°) suggests a hydrophobic surface, often limiting water interaction but reducing fouling when dealing with non-aqueous substances. So, the contact angle serves as a key indicator of surface energy, porosity, and roughness, directly influencing the membrane's filtration performance (W. Zhang et al., 1989).

4.3.5 Morphology

The morphology of the membranes was analyzed using Scanning Electron Microscopy (SEM) with a high-resolution Schottky Environmental Scanning Electron Microscope, equipped with X-Ray Microanalysis and Electron Backscattered Diffraction (EBSD) capabilities (FEI Quanta 400 FEG ESEM / EDAX Genesis X4M). This advanced imaging technique enables a detailed examination of the surface and structural characteristics of the membranes. To enhance the conductivity of the samples during SEM analysis, a thin film of gold/palladium (Au/Pd) was deposited on the membrane surfaces using a sputtering method. This process was carried out with the SPI Module Sputter Coater for samples identified as having low conductivity, ensuring optimal imaging conditions. The sputtering was conducted for a duration of 80 seconds at a current of 15 mA, within an argon atmosphere, to achieve a uniform coating that improves electron emission during SEM imaging. For the cross-sectional characterization of the membranes, the samples were prepared by cutting them under cryogenic

conditions, utilizing liquid nitrogen to ensure minimal thermal damage and preserve the structural integrity of the membranes. This technique allows for a clear view of the internal layers and interfaces within the membrane structure. The SEM images obtained were then analyzed using ImageJ software, a powerful tool for image processing and analysis. This analysis involved measuring the average membrane thickness based on ten individual measurements, following the methodology established in previous studies (Ribeiro et al., 2022). By employing this rigorous analytical approach, the study aims to provide comprehensive insights into the morphological features and thickness uniformity of the fabricated membranes, which are crucial for understanding their performance in water treatment applications.

4.3.6 Thermal decomposition

Thermal decomposition behavior of the membranes was studied using thermogravimetric analysis (TGA) and differential thermogravimetric analysis (DTG). These methods provide insight into the thermal stability and decomposition pathways of polymeric and composite membranes. TGA measures the mass loss of a sample as it is heated, allowing the detection of thermal events such as degradation, evaporation of volatile components, or structural changes. The addition of CNTs or other fillers can affect the thermal properties of membranes, improving or reducing their thermal stability. In this study, the analyses were carried out using a TA Instruments SDT650 analyzer. Membrane samples were heated from 50 to 950 °C at a constant heating rate of 10 °C per minute under an inert nitrogen atmosphere to avoid unwanted oxidation during the measurements. The TGA curve provides information about the onset and range of decomposition, while the DTG curve helps identify specific decomposition peaks, which can be attributed to the breakdown of different materials, such as the polymer matrix, additives, or embedded CNTs. These thermal decomposition characteristics are essential to understanding the behavior of the membranes under operational conditions and the influence of the incorporated materials on thermal stability (Mishra et al., 2016).

4.4 Intensified filtration experiments of CNMs

The continuous process will be carried out in the system assembled based on the Ribeiro et al., 2022, shown in Figure 7(a), which is a jacketed reactor adapted from a distillation tower.

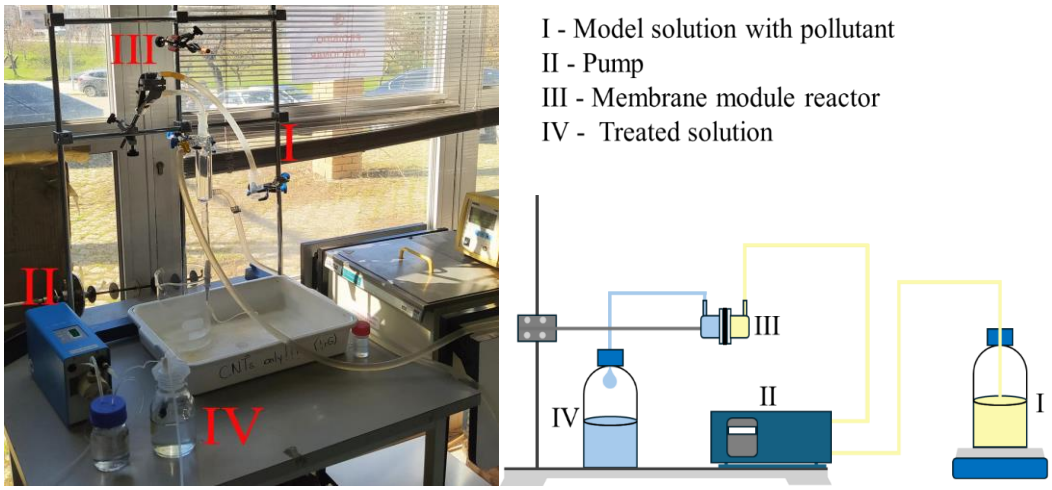

Figure 7. (a) Real continuous system (b) Schematic of the continuous system

Following the scheme in Figure 7b, (I) the flask loaded with model solution remained stirring throughout the experiment. (II) The HPLC pump (model) with a flow set to 1 mL min^{-1} was responsible for pumping the liquid through a heated column to heat it to 80 °C. For this purpose, the recirculation bath had the temperature adjusted to 82 °C to ensure the desired temperature upon entering the reactor. The composite membrane was placed inside the reactor shown in (III), Figure 7b, and the reaction start was considered upon seeing the first liquid droplet on the permeating side of the membrane. (IV) Samples were collected periodically in times of 0, 60, 120, 240, 360, and 480 min. The permeate flux was monitored along the reaction, and calculated according to Equation 10,

$$J = \frac{\Delta W}{A \cdot \Delta t} \tag{9}$$

in which J_W is the permeate flux (L m^{-2} h^{-1}), ΔW is the mass of solution that passes through the membrane, A is the effective area of the membrane (m^2), and Δt is the sampling time (min). The pollutant mass removal rate was calculated based on Equation 5,

$$m_{Removed} = J_W \cdot ([SMX]_i - [SMX]_o) \tag{10}$$

In which $[SMX]_i$ is the concentration of SMX in the reactor inlet, and $[SMX]_o$ is the concentration of SMX in the reactor outlet. Pure filtration experiments and H_2O_2 decomposition experiments were performed in the absence of H_2O_2 and pollutants, respectively. For the experiments, the flask containing the model solution was loaded with

SMX (10 µg mL-1) and a stoichiometric amount of H_2O_2 (44.3 µg mL^{-1}), calculated based on Equation 9. The model solution pH was adjusted to 3.5 to meet the optimized conditions for hydroxyl radical formation from H_2O_2.

$$C_{10}H_{11}N_3O_3S + 33\ H_2O_2 \rightarrow 10\ CO_2 + 36\ H_2O + 3\ HNO_3 + H_2SO_4 \quad (11)$$

The following Table 8 shows the separation of the continuous experiments carried out with each membrane.

Membranes	**Intensified filtration (CWPO)**	**Pure filtration**	**H_2O_2 Decomposition**
PVP/PVDF@CNT	Flow: 1 ml min^{-1} [SMX]: 10 µg mL^{-1} [H2O2]: 44.3 µg mL^{-1} Temperature: 82ºC pH: 3.5 Time online: 8h	Flow: 1 ml min^{-1} [SMX]: 10 µg mL^{-1} Temperature: 82ºC pH: 3.5 Time online: 8h	Flow: 1 ml min^{-1} [H2O2]: 44.3 µg mL^{-1} Temperature: 82ºC pH: 3.5 Time online: 8h
PVP/PVDF@CNTW			
PVP/PVDF@IO/Al_2O2			
PVP/PVDF			

Table 8: Parameters for Intensified filtration (CWPO), Pure filtration and H_2O_2 decomposition tests.

4.5 Analytical technics

4.5.1 SMX concentration by HPLC system

Following the methodology adapted from previous studies carried out by the group (A. S. Silva et al., 2023). The concentration of sulfamethoxazole (SMX) was monitored during the reaction using a Jasco HPLC system at a wavelength of 254 nm (UV-2075 Plus detector). For this determination, a BiPhenyl column (BPH 5 µm 150 x 2.1 mm) and 0.3 mL min^{-1} flow (PU-2089 Plus) of an A: B mixture of acetonitrile (A) and ultrapure water acidified with 0.1 *wt.*% formic acid (B) was used. The readings were performed in a 9-minute isocratic run (10:90).

4.5.2 H_2O_2 concentration by spectrophotometer

The concentration of H_2O_2 was followed by adapting a methodology used in previous works. In brief, a 0.5 mL reaction sample was added into a 5 mL volumetric flask previously loaded with 0.1 mL $TiOSO_4$ and 1 mL H_2SO_4 (0.5 M). The resultant mixture was analyzed at 405 nm using a spectrophotometer T70 from PG Instruments Ltd. (Lutterworth, United Kingdom) group (A. S. Silva et al., 2023).

5 RESULTS AND DISCUSSION

5.1 CNT production

The production of CNTs was carried out in 5 batches, as shown in Table 9. In total, 8,9838 g of nanotubes were produced for this work. The process proceeded as expected, achieving an average production efficiency of 35,87% in converting the polymeric material into CNTs through the CVD process, which is consistent with results from other studies. Additionally, 2,5221 g of CNTs were subjected to acid washing with H_2SO_4, yielding 1.4668 g of CNTW, corresponding to a material recovery efficiency of 58,16%, which also aligns with previous research findings, where the average production and purification efficiencies were within the expected range for CNTs made from LDPE, which is an advantage when choosing this type of material (Roman, De Grande Piccinin, et al., 2023).

Production	Catalyzer mass (g)	Polymer mass (g)	CNT (g)	Efficiency
1	1.0044	5.0053	1.7358	34.68%
2	1.0059	5.0089	1.9037	38.01%
3	1.0019	5.0036	1.8000	35.97%
4	1.0010	5.0156	1.7622	35.13%
5	1.0190	5.0117	1.7821	35.56%

Table 9. Results of CNT productions.

5.2 CNM production

The production of catalytic nanocomposite membranes was carried out in 14 batches, as shown in Table 10 below, with 2 batches for PVP/PVDF@CNT, 2 for PVP/PVDF@ IO/Al_2O_3, 4 for PVP/PVDF, and 6 for PVP/PVDF@CNTW. The higher number of batches for the basic PVP/PVDF membrane is related to the lower yield of material at the end of production, generating only 2 membranes per batch. On the other hand, the average number of membranes produced per batch for the other types was 3. However, half of the PVP/PVDF@CNTW batches failed, specifically batches 3*, 5*, and 8*. This occurred during the stirring stage of the polymeric material mixture with a magnetic stirrer in a flask kept in an oil bath at 40°C for 48 hours. At times, the magnetic stirrer stopped agitating the mixture, causing condensation to form on the perforated plastic film covering the flask. This condensation dripped directly onto the material, causing it to harden and coagulate prematurely. From this, it was understood that the magnetic stirrer must operate at a low frequency (90 to 120 rpm) to continuously stir the

viscous material without moving off-center during the 48-hour process. Another adjustment was to replace the perforated film covering the flask every 3 hours during the day to prevent moisture accumulation and avoid droplets falling into the polymer mixture.

Production	Membrane	PVP (g)	NMP (g)	CNT (g)	PVDF (g)	Mass (g)
1	PVP/PVDF@CNT	0.0712	6.18	0.2352	1.0710	7.56
2*	PVP/PVDF@CNTW	0.0750	6.18	0.2416	1.0999	7.60
3*	PVP/PVDF@CNTW	0.0702	6.18	0.2371	1.0741	7.56
4*	PVP/PVDF	0.0719	6.18	0	1.0757	7.33
5*	PVP/PVDF@CNTW	0.0699	6.18	0.2343	1.0741	7.56
6	PVP/PVDF	0.0733	6.18	0	1.0757	7.33
7	PVP/PVDF@IO/Al_2O_3	0.0755	6.18	0	1.0830	7.34
8*	PVP/PVDF@CNTW	0.0787	6.18	0.2357	1.0709	7.57
9	PVP/PVDF@CNTW	0.0753	6.18	0.2339	1.0717	7.56
10	PVP/PVDF@CNT	0.0703	6.18	0.2350	1.1822	7.46
11	PVP/PVDF@IO/Al_2O_3	0.0784	6.18	0	1.1985	7.46
12	PVP/PVDF	0.0743	6.18	0	1.1505	7.40
13	PVP/PVDF@CNTW	0.0755	6.18	0.2345	1.0733	7.56
14	PVP/PVDF	0.0745	6.18	0	1.0713	7.33

*Failed productions

Table 10. Membrane production results.

5.3 Characterization of the materials

5.3.1 Textural

Figure 8 shows the N_2 adsorption-desorption isotherms obtained for the membranes. The results demonstrated that the membranes did not significantly develop micro and mesoporosity, which is the typical range of porosities analyzed by this technique (Li et al., 2019).

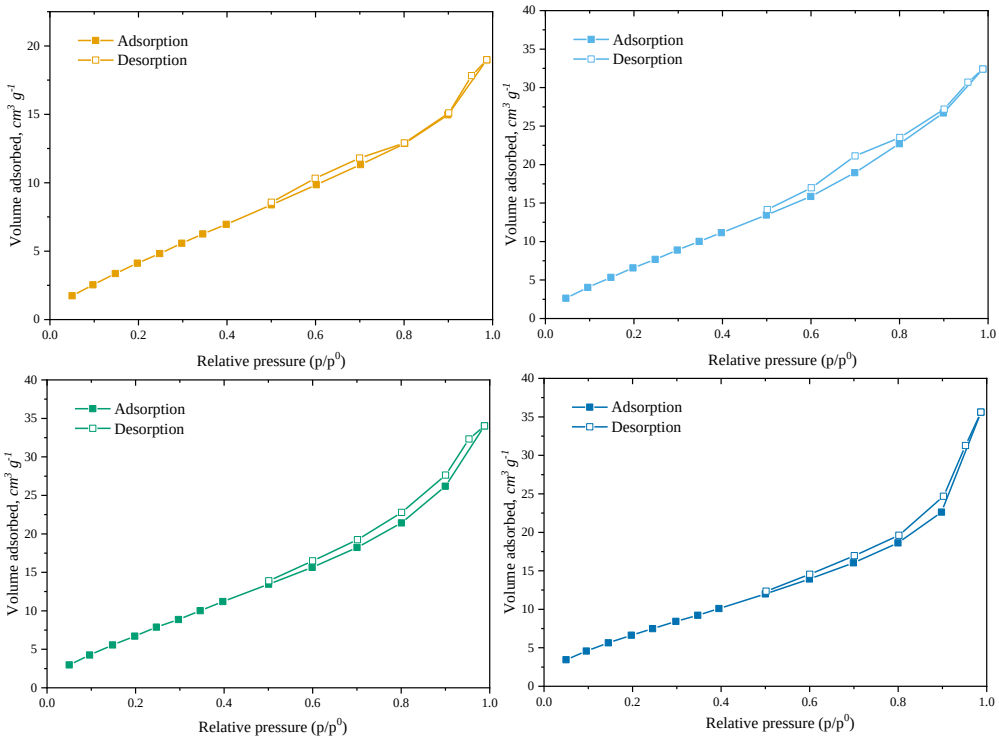

Figure 8: Adsorption-desorption isotherms.

Table 11 shows the results obtained for surface area and total pore volume, along with overall porosity, bubble point and contact angle.

Membrane	S_{BET} ($m^2\ g^{-1}$)	V_T ($mm^3\ g^{-1}$)	Porosity (%)	Contact angle (°)	d_{pore} (µm)
PVP/PVDF	22	0.0289	84	55	11
PVP/PVDF@IO/Al_2O_3	34	0.0494	84	73	10
PVP/PVDF@CNT	34	0.0516	70	88	4
PVP/PVDF@CNTW	29	0.0537	74	87	5

Table 11. Membrane texture and morphology results.

The incorporation of filler materials into the polymeric membrane led to a notable increase in surface area. This modification is primarily attributed to the addition of CNTs and

the CVD catalyst, which influence the dispersion and interaction between these solid materials and the casting solution. These interactions affect the solvent and non-solvent exchange during the membrane's porous structure formation, leading to changes in porosity and an increase in surface area. The specific textural properties of the filler materials play a significant role in this transformation. Consistent with these findings, other studies have also observed an enhancement in surface area when CNTs are incorporated into polymeric membrane structures, highlighting the impact of nanomaterial additives on membrane morphology and performance. (Ji et al., 2016).

The overall porosity was assessed using a gravimetric method, and the results, shown in Table 11, reveal that the incorporation of filler materials into the membrane composition led to a reduction in porosity. This reduction is likely due to the agglomeration of the materials into bundles or the formation of micro voids. The membrane prepared with the CVD catalyst exhibited the smallest decrease in porosity, which can be attributed to the lower amount of solid material used (0.089g). This specific amount of CVD catalyst was selected to match the metal content found in the CNT membrane, as determined by previous characterization studies (Diaz de Tuesta et al., 2023). Interestingly, the porosity of the PVP/PVDF@CNTW membrane was higher than that of the PVP/PVDF@CNT membrane, likely due to the surface chemistry changes that the CNTs underwent during the purification process. Similar observations regarding the decrease in overall porosity with the addition of filler material in composite membranes have been reported in other studies.

The membrane surface wettability was investigated by measuring the static water contact angle. The contact angle was measured using the equipment's built-in software, and the results are shown in Table 11. The result showed that blank membrane is highly hydrophilic, which is related to the presence of PVP in the membrane formulation (T. L. S. Silva et al., 2015b). Several works have already studied the incorporation of PVP in PVDF membrane to increase hydrophilicity and improve water compatibility (Mavukkandy et al., 2018) (C. Wang et al., 2019) (Purnawan et al., 2021). In this work, composite membranes increased the contact angle when filled with CVD catalyst (73°), pristine CNTs (88°), and purified CNTs (87°) compared to PVP/PVDF membrane (55°). The increase in water contact angle correlates to the hydrophilic/hydrophobic nature of the materials used to fabricate the composite membranes. Furthermore, the literature suggests that increased roughness due to the incorporation of a solid powder in composite membranes can affect the water contact angle (Purnawan et al., 2021). The highest increase in water contact angle observed for PVP/PVDF@CNT compared to PVP/PVDF@IO/Al_2O_3 is related to the hydrophobic nature of CNTs and the mild hydrophilic

nature of CVD catalyst. Despite the increase in contact angles observed upon modification, the composite membranes still have a higher hydrophilic character, which is of utmost importance considering the utilization of the membranes for wastewater treatment purposes (Guo et al., 2015).

The largest pore size (d_{pore}) of the membranes, determined using the bubble point method, highlighted the effect of the filling materials and their surface chemistry on membrane structure. Notably, incorporating these materials led to a reduction in the largest pore size across all samples, with the most significant decrease observed in membranes containing CNTs. The smallest pore size, approximately 4.5 µm, was recorded for the membrane containing purified CNTs, CNTW@IO/Al_2O_3. This reduction in pore size when CNTs are incorporated aligns with findings from other studies, demonstrating the impact of CNT loading on membrane morphology. (T. L. S. Silva et al., 2015b) .

5.3.2 Morphology

The SEM images recorded for all membranes are shown in Figure 9. The result obtained for the surface analysis for PVP/PVDF (Figure 9b) and PVP/PVDF@IO/Al_2O_3 (Figure 9d) composite membranes revealed both membranes with smooth surfaces. The backscattered electron imaging (BSE) performed in both samples revealed a porous network inside the membranes, as shown in Figures 9a and 9c. The images do not allow determining precisely the average membrane pore size but corroborate with previous results showing that PVP/PVDF@IO/Al_2O_3 have smaller pores (d_{pore} obtained for PVP/PVDF@IO/Al_2O_3 is 1 µm smaller than d_{pore} from PVP/PVDF membrane). The BSE results revealed a pore size smaller than PVDF/PVP@IO/Al_2O_3 and PVP/PVDF membranes, which was also confirmed with d_{pore} measurements (Table 11).

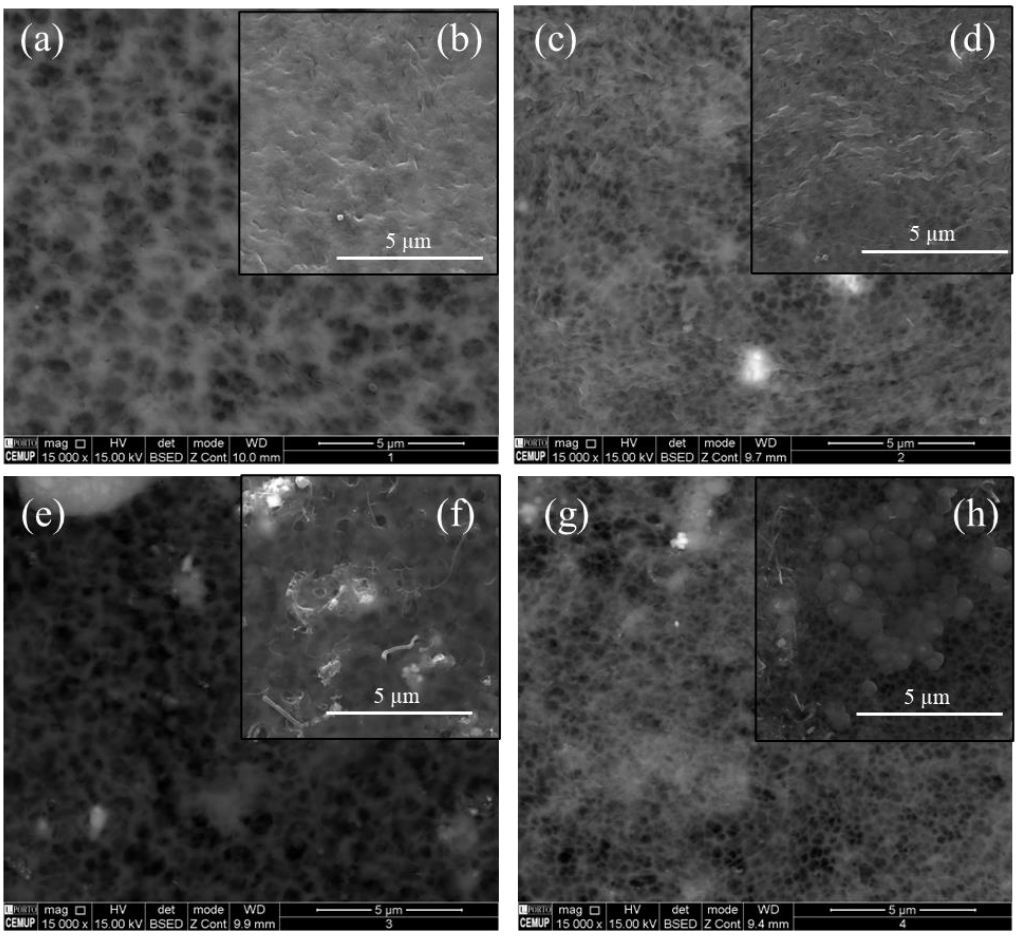

Figure 9. SEM images of (a,b) PVP/PVDF, (c,d) PVP/PVDF@IO/Al2O3, (e,f) PVP/PVDF@CNT, and (g,h) PVP/PVDF@CNTW. Figures (a,c,e,g) are from the BSE mode and figures (b,d,f,h) from the SEM mode.

The EDS result recorded for the samples revealed the presence of carbon and fluor in the PVP/PVDF membrane, and the presence of metals (Al, Fe) and oxygen in PVP/PVDF@IO/Al_2O_3 due to the utilization of iron oxide catalyst for its preparation (Figure 10). The Au and Pd signal observed in EDS comes from the coating performed to increase the sample conductivity so the images could be acquired in SEM.

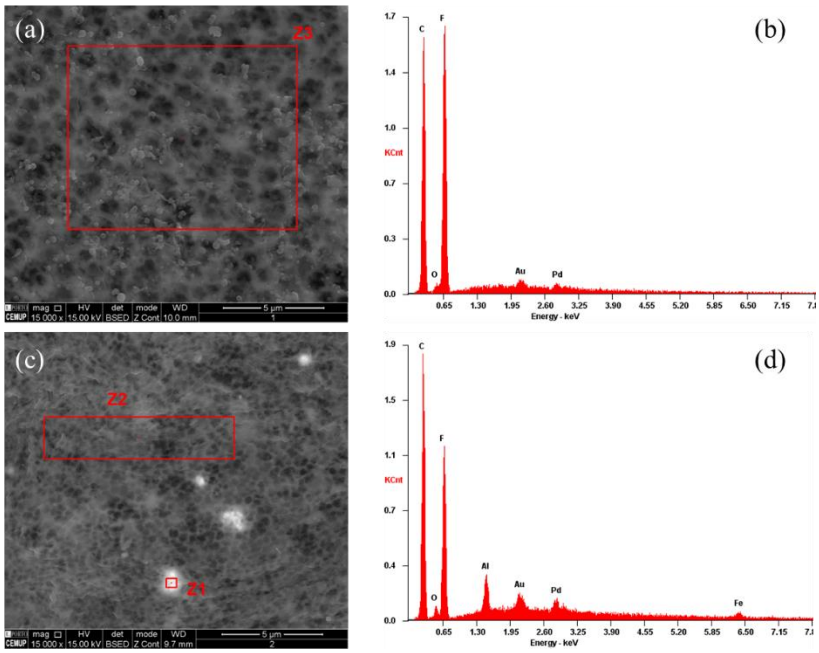

Figure 10. SEM and EDS results obtained for membrane (a,b) PVP/PVDF and (c, d) PVP/PVDF@Al2O3. Figures (a,c) are from SEM and Figures (b,d) are from EDS results.

Figure 11 clearly shows the presence of CNTs on the surface of both membranes. The sample PVP/PVDF@CNT (Figure 11a) showed the CNTs more dispersed in the sample compared to PVP/PVDF@CNTW (Figure 11b), which can be related to the highest compatibility of the CNT with no purification compared to the purified one. The poor dispersibility of CNTs in the polymeric membrane can be confirmed in Figure 11b, in which one can see the CNTs cluster in the left central side of the image.

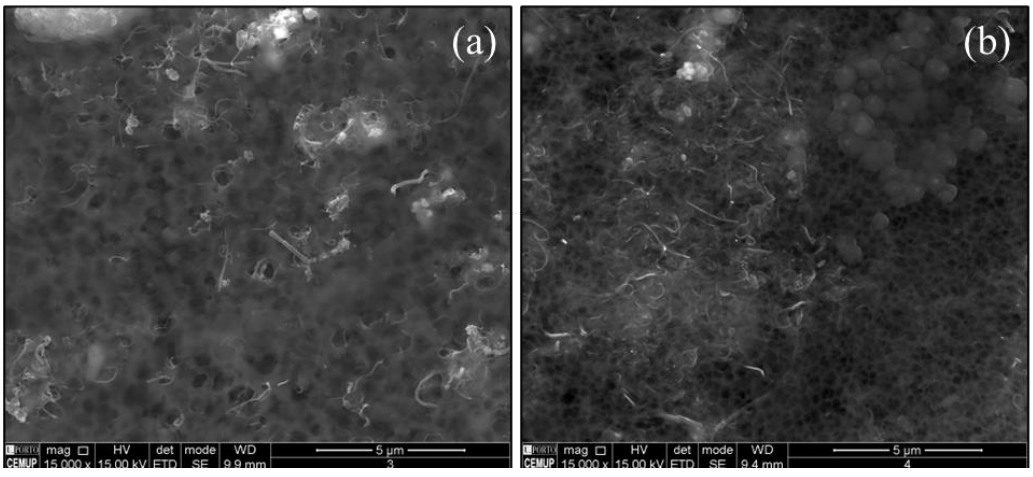

Figure 11. SEM images from samples (a) PVP/PVDF@CNT and (b) PVP/PVDF@CNTW.

The BSE result obtained for the membranes also showed how efficient the acid washing procedure is to remove metals from CNTs, since the amount of metal in the membrane clearly changed comparing Figure 12 a and c (SE mode) with Figures 12 b and d (BSE mode).

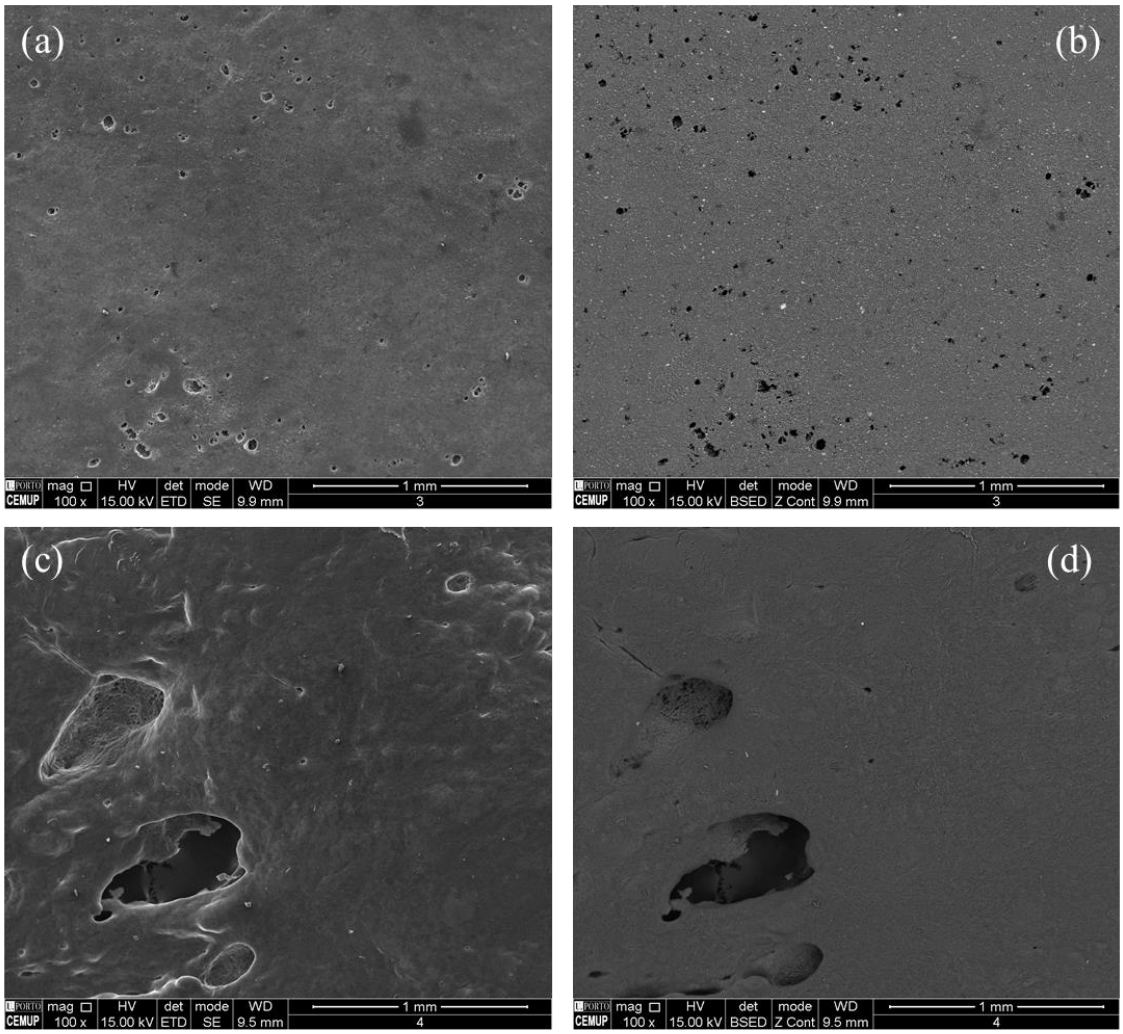

Figure 12. S10 SEM images of samples (a,b) PVP/PVDF@CNT and (c,d) PVP/PVDF@CNTW. Figures (a,c) were recorded in SE mode and Figures (b,d) were recorded in BSE mode.

The results obtained for the cross-section of PVP/PVDF@CNT, which showed more compatibility between additive and polymeric matrix, are shown in Figure 13. The result demonstrates that membrane thickness is about 100 ± 8 μm, which is close to the desired considering the synthesis procedure. Figure 13b confirmed the results observed previously with BSE, in which the pore structure inside the membrane and the smooth surface can be observed. The presence of pores inside the membrane and the absence of them on its surface is related to the knife-casting technique used to prepare the membrane. The uniform CNT distribution inside the polymeric structure can be confirmed with images from the top (Figure 13c), middle (Figure 13d), and lower (Figure 13e) regions of the membrane cross-section.

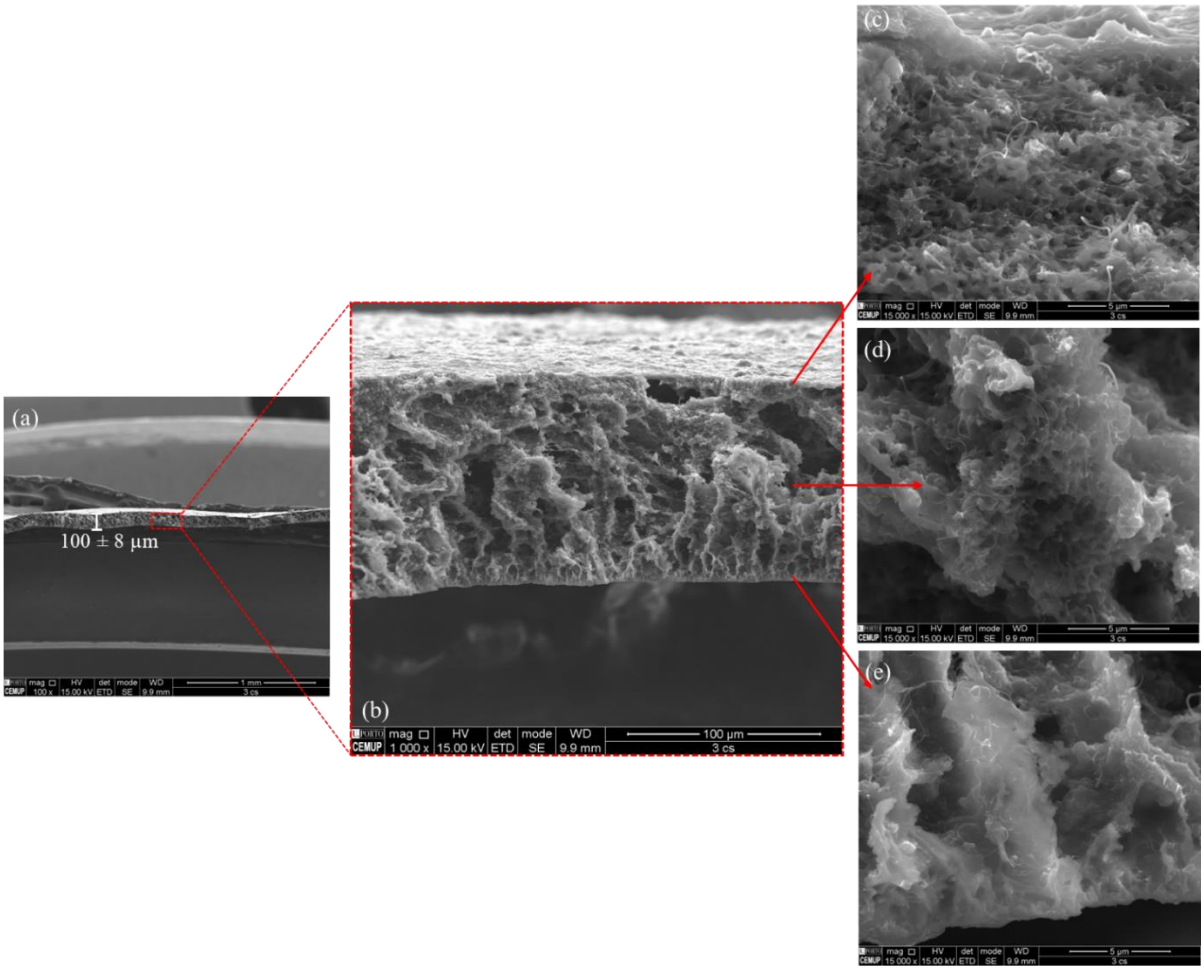

Figure 13. SEM image of the cross-section of PVP/PVDF@CNT (cut under cryogenic conditions). (a) whole membrane cross-section, (b) zoom in the pore network, (c) upper, (d) middle, and (e) lower regions of the zoomed membrane showing CNT distribution.

5.3.3 Thermogravimetric (TGA) and differential thermogravimetric (DTG)

The results obtained in TGA and DTG are shown in Figure 14 (N_2) and Figure 15 (air). The results demonstrate that all membranes have a thermal stability up to *ca.* 300 °C. The main mass loss peaks observed for the different samples were correlated with the filling material, with significant differences. For the blank membrane (Figure 14a) the mass loss peak was ca. 477 °C, which agrees with the literature (de Jesus Silva et al., 2020); and represents the PVDF decomposition. Another peak is observed in the PVP/PVDF membrane around 390 °C, ascribed to the thermal decomposition of PVP (T. L. S. Silva et al., 2015b). The addition of the metal catalyst in the polymeric membrane (PVP/PVDF@IO@Al_2O_3) caused the early degradation of the PVDF polymer since the mass loss peak was shifted to the left (*ca.* 370 °C; Figure 14b). The phenomenon is related to the metal-polymer interaction that catalyzes the thermal degradation under certain conditions (Bustamante-Torres et al., 2021; S. Lee et al.,

2020). The metal particles from CNT@IO/Al_2O_3, given that it is not purified, present in PVP/PVDF@CNT also affected the thermal decomposition of this membrane, shifting the two mass loss peaks to *ca.* 390 °C and 438 °C, ascribed to PVP and PVDF polymer degradation (Figure 14c). Lastly, the membrane prepared with the purified CNT (PVP/PVDF@CNTW; Figure 14d) demonstrated a thermal behavior closer to the original membrane with the main mass loss peak for PVDF being observed at *ca.* 465 °C. The final mass losses observed in an inert atmosphere agree with the literature, resulting in *ca.* 60 *wt.*% for membranes prepared with additives (Ribeiro et al., 2022).

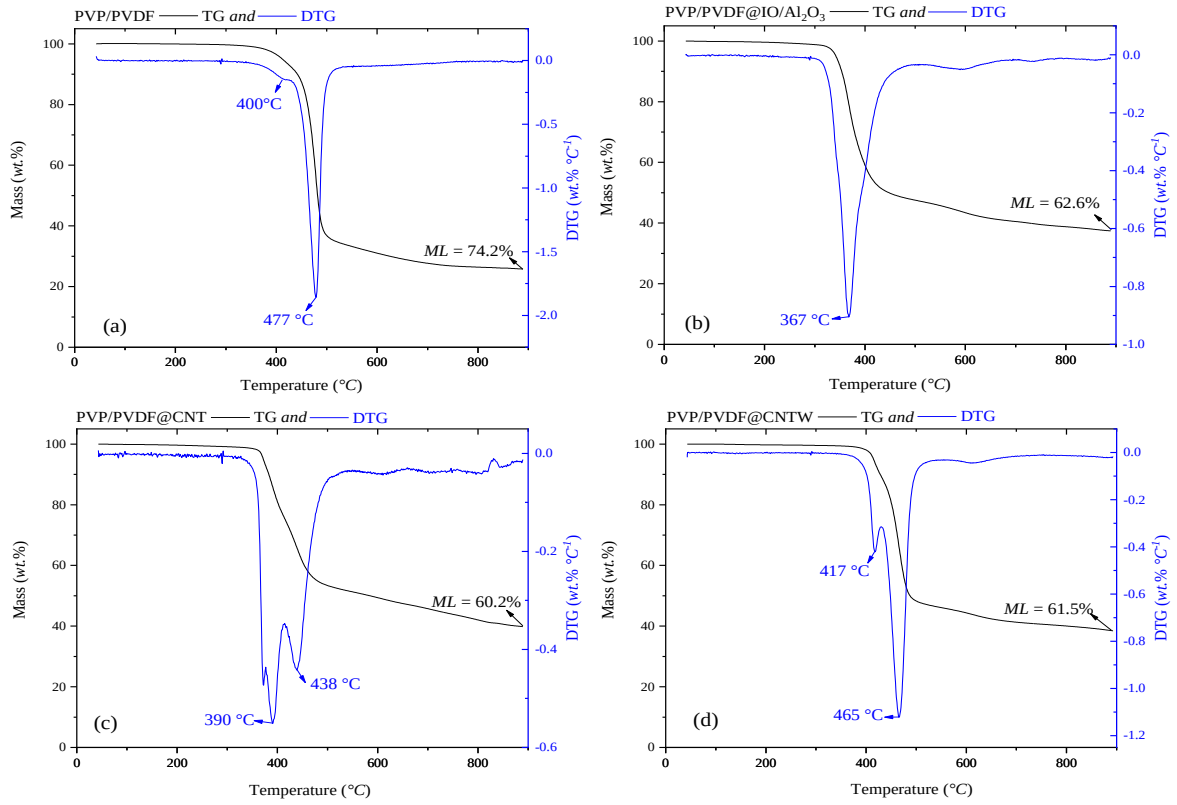

Figure 14: TGA results in N_2 atmosphere for (a) PVP/PVDF, (b) PVP/PVDF@IO/Al_2O_3, (c) PVP/PVDF@CNT, and (d) PVP/PVDF@CNTW.

The results obtained for TGA in air (Figure 15) revealed a mass loss peak (*ca.* 650 °C) ascribed to the degradation of the CNTs incorporated in the polymeric matrix (Figure 15c and Figure 15d) (Diaz de Tuesta et al., 2023).

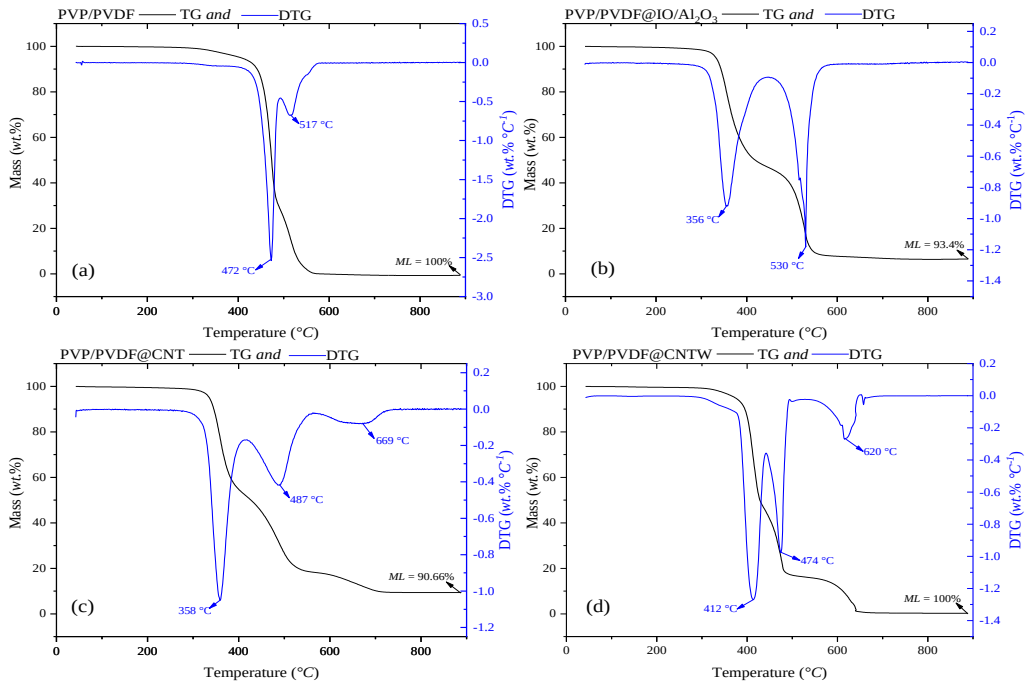

Figure 15. S11. TG and DTG curves in air for (a) PVP/PVDF, (b) PVP/PVDF@IO/Al2O3, (c) PVP/PVDF@CNT, and (d) PVP/PVDF@CNTW

Elemental analysis of the membranes was performed, with values calculated as 100 minus the sum of C, H, N, S, O, and ash content (ash content was determined using TG analysis in air, as shown in Figure 15). The elemental composition (C, H, N, S, and O) for the membranes is detailed in Table 12. The data indicate an increase in carbon content in the composite membranes containing purified CNTs compared to the pristine membrane, with 49% carbon in PVP/PVDF@CNTW versus 42% in PVP/PVDF. No significant changes were observed for the other elements analyzed, including oxygen. The remaining 25-27% in all membranes is primarily attributed to fluoride content, consistent with findings by Gayatri et al., 2024.

Membrane	C (wt.%)	H (wt.%)	N (wt.%)	S (wt.%)	O (wt.%)	Remaining * (wt.%)
PVP/PVDF	41.02±0.12	3.00±0.03	0.71±0.21	0.00±0.00	27.71±0.30	27.56
PVP/PVDF @IO/Al_2O_3	38.02±0.62	2.77±0.03	0.37±0.04	0.00±0.00	27.82±0.52	24.42
PVP/PVDF @CNT	41.88±0.14	2.54±0.02	0.62±0.01	0.00±0.00	22.98±0.25	22.64
PVP/PVDF @CNTW	49.10±0.10	2.51±0.01	0.53±0.01	0.00±0.00	21.89±0.23	25.97

Table 12. Elemental analysis of the membranes. *Calculated as 100-C-H-N-S-O-ashes (ashes determined by TG analysis in air, Figure 15)

5.1 Liquid-phase reactions

5.1.1 Pure filtration results and H_2O_2 decomposition ability

The results of the pure filtration experiments for all membranes are presented in Figure 16a. As shown, the membranes exhibited generally low filtration performance. Among them, the PVP/PVDF@CNT membrane demonstrated the highest initial SMX removal capacity, reaching its peak within the first hour of operation. However, the membrane's performance declined rapidly as the CNTs became saturated; the SMX removal efficiency dropped to approximately 20% between 2h-6h and further declined to nearly 0% by the 8h mark. The other membranes tested showed even lower filtration efficiency, with SMX removal rates below 10%.

The membrane's ability to decompose hydrogen peroxide under continuous flow conditions was evaluated, and the results are depicted in Figure 16b. The blank (unmodified) membrane exhibited minimal activity, with H_2O_2 decomposition rates remaining below 1%. In contrast, the membrane incorporating the CVD catalyst (IO/Al_2O_3) showed improved performance, achieving hydrogen peroxide decomposition rates of around 20-30% over the course of the 8h experiment.

Membranes containing CNTs displayed significantly higher hydrogen peroxide decomposition rates, with the composite membranes achieving 80-90% decomposition throughout the 8h testing period. No substantial difference was observed between the membranes containing synthesized and purified CNTs, indicating that the presence of CNTs is the primary factor driving catalytic activity. This is further supported by the noticeable

difference in performance between the CVD-catalyst composite membrane and those enriched with CNTs, highlighting that CNTs are the key active component in the composite membranes. Previous studies have also demonstrated the catalytic activity of carbon-based phases in hydrogen peroxide decomposition. (A. S. Silva et al., 2023; A. S. Silva et al., 2024).

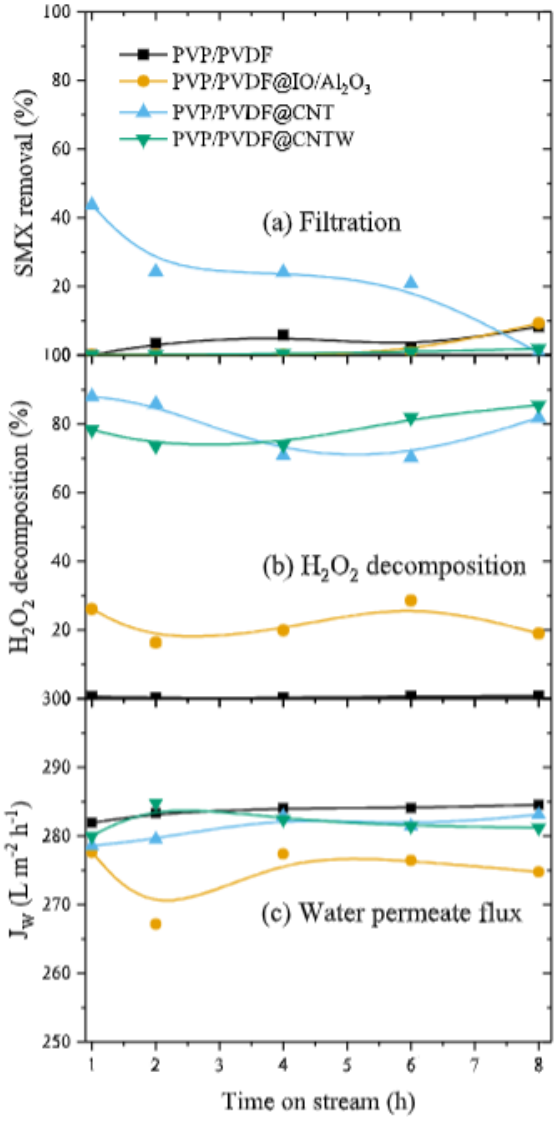

Figure 16: (a) Pure adsorption (filtration), (b) pure H_2O_2 decomposition and (c) water permeate flux during CWPO-enhanced and pure filtration considering the different membranes upon time on stream. Conditions : Q = 1 mL min^{-1}, T = 80 °C, pH_0 = 3.5, [SMX] = 20 mg L^{-1}, $[H_2O_2]_0$ = 44.3 mg L^{-1}. Adsorption and H_2O_2 decomposition were carried out in the absence of H_2O_2 and SMX, respectively.

5.1.2 CWPO intensified filtration

The results of the CWPO-enhanced filtration experiments are presented in Figure 17. The blank membrane (PVP/PVDF) exhibited minimal SMX removal, with efficiency levels remaining below 10% (Figure 17a). This behavior is consistent with the results obtained during the pure filtration tests (Figure 16a), suggesting that the membrane's baseline capacity for SMX removal is inherently low. Similarly, the blank membrane showed no significant hydrogen peroxide (H_2O_2) consumption (Figure 17b), aligning with its performance during the pure H_2O_2 decomposition experiments (Figure 16b).

Incorporating the CVD catalyst (IO/Al_2O_3) into the membrane composition resulted in a slight improvement, with SMX removal rates fluctuating between 10-20% over the 8h operation period. However, a decline in SMX removal efficiency was observed towards the end of the experiment (from 6 to 8 hours), where it decreased from 20% to 10%. This drop correlated with a reduction in H_2O_2 consumption (Figure 17b), indicating a diminished catalytic performance as the operation progressed. Overall, both the PVP/PVDF and PVP/PVDF@IO/Al_2O_3 membranes demonstrated limited efficacy in SMX removal, whether through pure filtration or CWPO-enhanced processes.

Conversely, the incorporation of CNTs into the membranes significantly improved SMX removal performance. From the 4 hour mark onward, the CNT-enriched composite membranes consistently achieved high SMX removal rates of approximately 85% for PVP/PVDF@CNT and 90% for PVP/PVDF@CNTW. These removal rates correspond to pollutant mass removal efficiencies of approximately 2451 and 2551 mg m^{-2} h^{-1}, respectively. Furthermore, the CNT-enriched membranes demonstrated a substantial increase in hydrogen peroxide decomposition, maintaining H_2O_2 consumption levels above 65% throughout the entire 8h operation period (Figure 17b). Notably, the water permeates flux (JW) remained stable during the operation, as illustrated in Figure 16c, indicating that the membranes maintained their structural integrity and filtration efficiency over time.

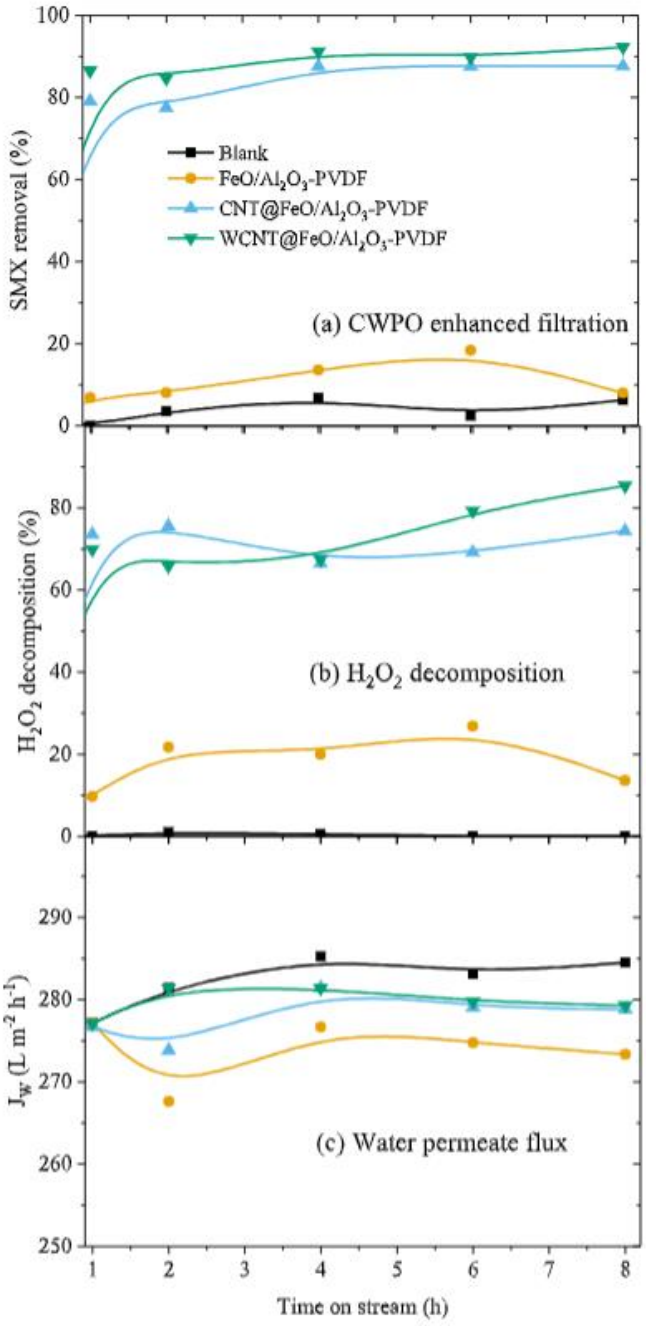

Figure 17: CWPO-enhanced filtration runs. Conversion of (a) SMX and (b) H_2O_2 considering the different membranes upon time on stream. Conditions: Q = 1 mL min^{-1}, [SMX] =10 mg L^{-1}, $[H_2O_2]_0$ = 44.3 mg L^{-1}, T = 80 °C, pH_0 = 3.5.

Similar results have been previously reported for composite polymeric membranes in AOPs-enhanced filtration. Ribeiro et al., 2022 reported a removal of 71% of venlafaxine (1.97 mg m^{-2} h^{-1}) with activated persulfate oxidation and CNT-enriched membranes, achieving a steady state after 5 h of reaction. Vieira et al., 2020 obtained 85-90% removal of three micropollutants (ciprofloxacin, enrofloxacin, and ofloxacin, equivalent to 2.56-2.72 mg m^{-2} h^{-}

[1]) using graphene oxide composite membranes for the activated persulfate oxidation, achieving a steady state after 2 h of operation. Nieto-Sandoval et al., 2023 reported steady state removals (after 3 h) of 89%, 92% and 72% for metoprolol, venlafaxine and diclofenac, respectively, using carbon nitride composite membranes in the photocatalytic oxidation whereas a blank membrane allowed removals below 5%. Ma et al., 2020 reported 65% removal of SMX after 100 min of operation for the peroxymonosulfate oxidation using CNT-enriched membranes.

Iron was measured in final sample and no metal was detected, showing that all membranes are stable for liquid-phase reactions in these conditions.

Furthermore, by evaluating the results of other studies that utilized CNTs in PVDF-based membranes for AOP applications (Table 13) and studies that used CNTs in CNMs to remove SMX via AOPs (Table 14), it is possible to draw promising comparisons with this research. The continuous removal of 80% to 90% of SMX during 2 and 8 hours of operation, respectively, appears promising, especially when compared to other works in terms of total operation time, removal rate, and concentrations of pollutant and reagent.

Reviewing other studies that also developed CNMs with CNT on a PVDF polymeric base in AOPs. For this, a search was conducted using the keywords "carbon AND nanotube AND pvdf AND membrane AND oxidation," yielding 32 studies on Scopus and 42 on Web of Science (WoS). Most of these studies focused on membranes applied in electrochemical processes, with only 12 studies specifically on PVDF@CNT membranes applied in advanced oxidation processes (AOPs). These studies are listed in Table 13. A search for studies that incorporated CNTs into membranes to enhance filtration through advanced oxidation processes (AOPs) was conducted using the keywords "carbon AND nanotube AND membrane AND oxidation AND SMX." This search yielded 12 studies, as listed Table 14. Specifically, 15 studies were identified on Web of Science (WoS) and 11 on Scopus, with the majority focusing on electrochemical applications

Author	Title	Membrane	AOP method and characteristics	Pollutant and concentration	Water matrix	Pollutant removal
An et al. (2023)	Well-defined Fe/Cu diatomic catalysts for boosted peroxymonosulfate activation to degrade organic contaminants	Fe/Cu DA -NC/PVDF membrane	Peroxymonosulfate (PMS) [80 g/L]	Sulfamethoxazole (SMX) [10 mg/L]	Deionized water	90% SMX After 1hr
Zhong et al. (2023)	Mo and N co-doped iron biochar materials activating peroxymonosulfate for enhanced degradation of bisphenol A: Mechanism discussion and practical application	Membrane Fe/Mo0,1-NC/PVDF	Peroxymonosulfate (PMS) [0,1 - 1 g/L]	Bisphenol A (BPA) [8 and 20 mg/L]	Ultrapure water Effluent water	99% BPA after 30 min 82.6% TOC After 1hr
B. Chen et al. (2022)	Novel catalytic self-cleaning membrane with peroxymonosulfate activation for dual-function wastewater purification: Performance and mechanism	MnO_2/C-CNT@PVDF membrane. manganese dioxide (MnO_2)/carboxyl functionalized carbon nanotube (C-CNT) composites were prepared	peroxymonosulfate (PMS) [0.25 – 1.0 g/L]	Rhodamine B (Rh B) [50 - 100 g/L]	Deionized water	99,5% after 3min
Ribeiro et al. (2022)	Synthesis of low-density polyethylene derived carbon nanotubes for activation of persulfate and degradation of water organic micropollutants in continuous mode	PVDF membranes were prepared with CNTs produced from 4 different metal substrates using Al_2O_3, Ni, Fe and/or Al).	Persulfate (SPS) [250 mg/L]	Venlafaxine [100 µg/L]	Surface water	99% after 1.5hr
Q. Xu et al. (2022)	Synergistic oxidation-filtration process of electroactive peroxydisulfate with a cathodic composite CNT-PPy/PVDF ultrafiltration membrane	Carbon nanotube cross-linked polypyrrole composite ultrafiltration membrane (CNT-PPy/PVDF)	electro-filtration activated peroxydisulfate (PDS) [50 mM]	Carbamazepine [All: 2 mg/L]	Deionized water	95% After 100min
Ye, Dai, Li, et al. (2021)	Lawn-like Co_3O_4@N-doped carbon-based catalytic self-cleaning membrane with peroxymonosulfate activation: A highly efficient singlet oxygen dominated process for sulfamethoxazole degradation	Co_3O_4@NCNTs/g-CN membrane made of nitrogen-doped carbon nanotubes with Co_3O_4, grown in-situ on gC_3N_4. CoxOy@CCNM achieved instantaneous antibiotic degradation efficiency under flow filtration	Peroxymonosulfate (PMS) [0.2 g/L]	Sulfamethoxazole (SMX) [10 mg/L]]	Deionized water	98,9% SMX after 20min

Ye, Dai, Wang, et al. (2021)	Investigation of catalytic self-cleaning process of multiple active species decorated macroporous PVDF membranes through peroxymonosulfate activation	Fe-Co@NC-CNTs/PVDF membrane	Peroxymonosulfate (PMS) [0.3 g/L]	Bisphenol A (BPA) [30 mg/L]	Deionized water	100% BPA after 40min
Ye, Li, Wang, Yan, et al. (2021)	MOFs derived 3D sea urchin-like carbon frameworks loaded on PVDF membranes as PMS activator for highly efficient bisphenol A degradation	carbon nanotube (CNT) frameworks encapsulated Co nanoparticles (ZIF-67/CNTs) through N-molecule assisted pyrolysis of ZIF-67, and then immobilized on PVDF membrane to obtain the catalytic membranes (ZIF-67/CNTs-II@PVDF).	Peroxymonosulfate (PMS) [100 mg/L]	Bisphenol A (BPA) [25 mg/L]	Deionized water	96.8% BPA after 40 min
Alpatova et al. (2015)	Composite polyvinylidene fluoride (PVDF) membrane impregnated with Fe_2O_3 nanoparticles and multiwalled carbon nanotubes for catalytic degradation of organic contaminants	polyvinylidene fluoride (PVDF) polymeric membranes with inclusion of Fe_2O_3 nanoparticles and multi-walled carbon nanotubes (MWCNTs)	Hydrogen peroxide (H_2O_2) [110 mg/L]	Cyclohexanoic (CHA) [5 mg/L] Humic acids (AHs) [5 mg/L]	Deionized water	48% do CHA after 24hr and 53% do AHs after 33h

Table 13. CNT CNMs based in PVDF applied in AOPs.

Author	Title	Catalytic membrane	AOP	Pollutant and concentration	Water matrix	Pollutant removal
L. Wang et al. (2024)	Fabrication of Fe-$CoTiO_3$/TiO_2/Ti catalytic membrane for peroxymonosulfate activation to efficient sulfamethoxazole degradation	Fe-doped Fe-$CoTiO_3$/TiO_2/Ti (FCTT) membrane in which TiO2 nanotubes were inserted	Peroxymonosulfate (PMS) [0.8 mM]	Sulfamethoxazole (SMX) [10 mg/L]	Deionized water Tap water River water	98% SMX 96,43% SMX 92,87% SMX All after <10min
Ma et al. (2024)	New insights into Co3O4-carbon nanotube membrane for enhanced water purification: Regulated peroxymonosulfate activation mechanism via nanoconfinement	Co3O4-in-CNT membrane	Peroxymonosulfate (PMS) [0.33 mM]	Sulfamethoxazole (SMX) [0,04 mM]	Deionized water	99,5% SMX After <1 min
R. Wang et al. (2024)	Non-radical mediated reduced graphene oxide/polypyrrole catalytic ceramic membrane-PDS system for source control of SMX	rGO/PPy CM membranes, reduced graphene oxide/polypyrrole (ceramics)	Peroxydisulfate (PDS) [0.5 mM]	Sulfamethoxazole (SMX) [10 ~ 50 µM]	Deionized water	95% After 10 min
Xia et al. (2023)	Effects of peroxide types on the removal performance and mechanism of sulfonamide antibiotics using graphene-based catalytic membranes	rGO/N-CNT membranes of reduced graphene oxide and nitrogen-doped	Peroxydisulfate (PDS) Peroxymonosulfate (PMS) Hydrogen peroxide (H_2O_2) All: [1mM]	Sulfamethoxazole (SMX) Sulfadiazina (SDZ) Sulfamerazina (SMR) Sulfametazina (SM2) All: [500 µg/L]	Deionized water Surface water	93% SMX 98% SDZ 99% SMR 90% SM2 After 10h
An et al. (2023)	Well-defined Fe/Cu diatomic catalysts for boosted peroxymonosulfate activation to degrade organic contaminants	Fe/Cu DA -NC/PVDF membrane.	Peroxymonosulfate (PMS) [2 g/L]	Sulfamethoxazole (SMX) [10 mg/L]	Deionized water	90% SMX After 1hr
Qian et al. (2022)	Carbonaceous composite membranes for peroxydisulfate activation to remove sulfamethoxazole in a real water matrix	Membrane composed of NG/rGO/CNTs.	Peroxydisulfate (PDS) [2 mM]	Sulfamethoxazole (SMX) [500 µg/L]	Deionized water Tap water Surface water Effluent from aerobic tank	23.03 mg/m²h 22.15 mg/m²h 7.32 mg/m²h 10.84 mg/m²h 3.95 mg/m²h After 24h

N. Lu et al. (2021)	ZIF-67 derived nanofibrous catalytic membranes for ultrafast removal of antibiotics under flow-through filtration via non-radical dominated pathway	CoxOy@CCNM membranes	Peroxymonosulfate (PMS) [1 ~ 4 mM]	Tetracycline (TC) Ciprofloxacin (CIP) Sulfamethoxazole (SMX) Todos: [30 mg/L]]	Deionized water	99.11% TC 9.08% CIP 99.38% SMX After <1min
Ye, Dai, Li, et al. (2021)	Lawn-like Co3O4@N-doped carbon-based catalytic self-cleaning membrane with peroxymonosulfate activation: A highly efficient singlet oxygen dominated process for sulfamethoxazole degradation	Co_3O_4@NCNTs/g-CN membrane made of nitrogen-doped carbon nanotubes with Co_3O_4	Peroxymonosulfate (PMS) [0.025 ~ 0.2 g/L]	Sulfamethoxazole (SMX) [10 mg/L]]	Deionized water	98.9% SMX After 20min
Ye, Wang, Li, Yang, et al. (2021)	2D confinement freestanding graphene oxide composite membranes with enriched oxygen vacancies for enhanced organic contaminants removal via peroxymonosulfate activation	FeCo@GCTs/GO membrane, developed a kind of novel lawn-like Fe2O3@Co0.08Fe1.92@nitrogen-doped reduced graphene oxide@carbon nanotube composites	Peroxymonosulfate (PMS) [0.2 g/L]	Sulfamethoxazole (SMX) [10 mg/L]	Deionized water	98% SMX After 30min
Qian et al. (2021)	The in situ catalytic oxidation of sulfamethoxazole via peroxydisulfate activation operated in a NG/rGO/CNTs composite membrane filtration	NG/rGO/CNTs composite membrane. Nitrogen-doped graphene (NG) was used as a modifier to increase catalytic activity with reduced graphene oxide (rGO) and carbon nanotubes (CNTs).	Peroxymonosulfate (PMS) [2 ~ 5 mmol/L]	Sulfamethoxazole (SMX) [500 μg/L]	Deionized water	21.7 mg/m²h 94% SMX After 140min
Sheng et al. (2020)	Reduced graphene oxide-based composite membranes for in-situ catalytic oxidation of sulfamethoxazole operated in membrane filtration	rGO/CNTs membrane made with graphene oxide and CNTs in a 3:1 ratio	Persulfate (PS)	Sulfamethoxazole (SMX) [500 μg/L]	Deionized water	77% SMX After 3h

Table 14. CNT CNMs studies applied in AOPs to remove SMX

6 CONCLUSIONS

The results obtained from the developed and tested CNMs for the CWPO in the filtration intensification process demonstrated significant efficiency in the degradation of the antibiotic SMX in a continuous flow dead-end system. The characterization of the membranes revealed that the distribution of filler materials, particularly CNTs, played a crucial role in the observed efficiency, especially in the membranes prepared with both unpurified and purified CNTs.

Morphological analysis using Scanning Electron Microscopy (SEM) showed a uniform distribution of CNTs within the polymeric matrix of the membranes, particularly in the PVP/PVDF@CNT, which favored catalytic performance. In contrast, the membrane with washed CNTs (PVP/PVDF@CNTW) exhibited a less homogeneous distribution, suggesting that the acid washing process may negatively influence the dispersion and interaction of the CNTs with the polymeric matrix.

Regarding the hydrogen peroxide decomposition capacity, the PVP/PVDF@CNT membrane proved to be the most efficient, maintaining H_2O_2 consumption above 80% during the 8 hour operation. This efficiency is attributed to the presence of CNTs, which emerged as the main active fraction of the membranes, corroborating previous studies that indicate the effectiveness of carbon phases in the catalytic decomposition of hydrogen peroxide. Furthermore, no significant iron leaching was observed in the samples, confirming the stability of the membranes and their feasibility for use without the need for acid treatment for CNT purification.

The CWPO-enhanced filtration tests demonstrated that the CNT-enriched membranes achieved an SMX removal of up to 90%, corresponding to a pollutant mass removal of up to 2551 mg m^2 h^{-1}. This highlights the potential of the developed membranes not only for physical filtration but also for the catalytic degradation of contaminants of emerging concern (CECs), promoting the purification of wastewater more efficiently.

Thus, the study confirms that the PVP/PVDF@CNT membranes have significant potential for application in treatment systems for contaminated water with emerging pollutants. The use of plastic waste as a source for CNT production illustrates the feasibility of integrating these materials into a circular economy, promoting the upcycling of plastic waste and contributing to environmental sustainability. In summary, it achieves to aim to develop and evaluate effective CNMs for removing CECs, validate their use as upcycling products, and reinforce their role in plastic waste recovery and reusing purified water.

7 FUTURE RESEARCH

- Exploration of Different Nanomaterials: Investigate the use of other types of nanomaterials, in addition to carbon nanotubes (CNTs), such as graphene or metal nanoparticles, in the fabrication of nanocomposite membranes. This could provide a comparative performance analysis regarding the degradation of emerging contaminants.
- Study of the Effect of Different Operational Conditions: Conduct studies on how operational conditions, such as temperature, pH, and H_2O_2 concentration, along with other Advanced Oxidation Processes (AOPs), may affect the efficiency of the membranes. Understanding these variables could optimize the performance of the membranes in oxidation processes.
- Long-Term Stability Analysis of the Membranes: Evaluate the stability and durability of the CNM membranes over a period longer than 8 hours under real operating conditions. This is crucial for understanding their applicability in long-term water treatment systems.
- Recovery and Reuse of Materials: Investigate methods to recover and reuse the CNTs and other membrane components after use, thus promoting a circular economy approach. This research could significantly contribute to sustainability. Additionally, testing the incorporation of residual polymers for the construction of CNTs and membranes could be beneficial.
- Evaluation of Other Classes of Contaminants: Expand testing to include a variety of emerging contaminants beyond sulfamethoxazole (SMX), such as other antibiotics or other CECs. This could help better understand the scope of membrane applications.
- Integration with Other Treatment Technologies: Explore the combination of nanocomposite membranes with other treatment technologies, such as photocatalysis, ozone oxidation, or electrochemical oxidation, to create hybrid treatment systems that further enhance the efficiency of contaminant removal.

8 REFERENCES

Ahmad, A. L., Abdulkarim, A. A., Ooi, B. S., & Ismail, S. (2013). Recent development in additives modifications of polyethersulfone membrane for flux enhancement. *Chemical Engineering Journal*, *223*, 246–267. https://doi.org/10.1016/J.CEJ.2013.02.130

Ajayan, P. M., Stephan, O., Colliex, C., & Trauth, D. (1994). Aligned Carbon Nanotube Arrays Formed by Cutting a Polymer Resin—Nanotube Composite. *Science*, *265*(5176), 1212–1214. https://doi.org/10.1126/science.265.5176.1212

Ali, S., Rehman, S. A. U., Luan, H. Y., Farid, M. U., & Huang, H. (2019). Challenges and opportunities in functional carbon nanotubes for membrane-based water treatment and desalination. *Science of The Total Environment*, *646*, 1126–1139. https://doi.org/10.1016/J.SCITOTENV.2018.07.348

Alpatova, A., Meshref, M., McPhedran, K. N., & Gamal El-Din, M. (2015). Composite polyvinylidene fluoride (PVDF) membrane impregnated with Fe2O3 nanoparticles and multiwalled carbon nanotubes for catalytic degradation of organic contaminants. *Journal of Membrane Science*, *490*, 227–235. https://doi.org/10.1016/j.memsci.2015.05.001

Al-Salem, S. M., Lettieri, P., & Baeyens, J. (2009). Recycling and recovery routes of plastic solid waste (PSW): A review. *Waste Management*, *29*(10), 2625–2643. https://doi.org/10.1016/j.wasman.2009.06.004

An, S., Wang, L., Li, G., Zhu, B., & Jin, Q. (2023). Well-defined Fe/Cu diatomic catalysts for boosted peroxymonosulfate activation to degrade organic contaminants. *Separation and Purification Technology*, *316*, 123827. https://doi.org/10.1016/j.seppur.2023.123827

Arvaniti, O. S., & Stasinakis, A. S. (2015). Review on the occurrence, fate and removal of perfluorinated compounds during wastewater treatment. *Science of The Total Environment*, *524–525*, 81–92. https://doi.org/10.1016/j.scitotenv.2015.04.023

Barrejón, M., & Prato, M. (2022). Carbon Nanotube Membranes in Water Treatment Applications. *Advanced Materials Interfaces*, *9*(1). https://doi.org/10.1002/admi.202101260

Bazargan, A., & McKay, G. (2012). A review – Synthesis of carbon nanotubes from plastic wastes. *Chemical Engineering Journal*, *195–196*, 377–391. https://doi.org/10.1016/J.CEJ.2012.03.077

Bila, D. M., & Dezotti, M. (2007). Desreguladores endócrinos no meio ambiente: efeitos e conseqüências. *Química Nova*, *30*(3), 651–666. https://doi.org/10.1590/S0100-40422007000300027

Bonchio, M., Syrgiannis, Z., Burian, M., Marino, N., Pizzolato, E., Dirian, K., Rigodanza, F., Volpato, G. A., La Ganga, G., Demitri, N., Berardi, S., Amenitsch, H., Guldi, D. M., Caramori, S., Bignozzi, C. A., Sartorel, A., & Prato, M. (2019). Hierarchical organization of perylene bisimides and polyoxometalates for photo-assisted water oxidation. *Nature Chemistry*, *11*(2), 146–153. https://doi.org/10.1038/s41557-018-0172-y

Bustamante-Torres, M., Romero-Fierro, D., Arcentales-Vera, B., Pardo, S., & Bucio, E. (2021). Interaction between filler and polymeric matrix in nanocomposites: Magnetic approach and applications. *Polymers*, *13*(17). https://doi.org/10.3390/polym13172998

Campanale, Massarelli, Savino, Locaputo, & Uricchio. (2020). A Detailed Review Study on Potential Effects of Microplastics and Additives of Concern on Human Health. *International Journal of Environmental Research and Public Health*, *17*(4), 1212. https://doi.org/10.3390/ijerph17041212

Carroccio, S. C., Scarfato, P., Bruno, E., Aprea, P., Dintcheva, N. T., & Filippone, G. (2022). Impact of nanoparticles on the environmental sustainability of polymer nanocomposites based on bioplastics or recycled plastics – A review of life-cycle assessment studies. *Journal of Cleaner Production*, *335*, 130322. https://doi.org/10.1016/j.jclepro.2021.130322

ChemSpider. (2024, February 28). *Search and share chemistry*. Https://Www.Chemspider.Com/.

Chen, B., Hu, X., Wang, J., Li, R., Shen, L., Xu, Y., Zhang, M., Hong, H., & Lin, H. (2022). Novel catalytic self-cleaning membrane with peroxymonosulfate activation for dual-function wastewater purification: Performance and mechanism. *Journal of Cleaner Production*, *355*, 131858. https://doi.org/10.1016/J.JCLEPRO.2022.131858

Chen, C., Chen, L., Zhu, X., & Chen, B. (2022). Graphene nanofiltration membrane intercalated with AgNP@g-C3N4 for efficient water purification and photocatalytic self-cleaning performance. *Chemical Engineering Journal*, *441*, 136089. https://doi.org/10.1016/J.CEJ.2022.136089

Chen, C., Lu, L., Fei, L., Xu, J., Wang, B., Li, B., Shen, L., & Lin, H. (2023). Membrane-catalysis integrated system for contaminants degradation and membrane fouling mitigation: A review. *Science of The Total Environment*, *904*, 166220. https://doi.org/10.1016/J.SCITOTENV.2023.166220

Cimmino, I., Fiory, F., Perruolo, G., Miele, C., Beguinot, F., Formisano, P., & Oriente, F. (2020). Potential Mechanisms of Bisphenol A (BPA) Contributing to Human Disease.

International Journal of Molecular Sciences, *21*(16), 5761. https://doi.org/10.3390/ijms21165761

Cruz-Alcalde, A., López-Vinent, N., Ribeiro, R. S., Giménez, J., Sans, C., & Silva, A. M. T. (2022). Persulfate activation by reduced graphene oxide membranes: Practical and mechanistic insights concerning organic pollutants abatement. *Chemical Engineering Journal*, *427*, 130994. https://doi.org/10.1016/J.CEJ.2021.130994

De Filpo, G., Pantuso, E., Armentano, K., Formoso, P., Di Profio, G., Poerio, T., Fontananova, E., Meringolo, C., Mashin, A., & Nicoletta, F. (2018). Chemical Vapor Deposition of Photocatalyst Nanoparticles on PVDF Membranes for Advanced Oxidation Processes. *Membranes*, *8*(3), 35. https://doi.org/10.3390/membranes8030035

de Freitas Batista, G., Roman, F. F., de Tuesta, J. L. D., Mambrini, R. V., Praça, P., & Gomes, H. T. (2022). Assessment of Pretreatments for Highly Concentrated Leachate Waters to Enhance the Performance of Catalytic Wet Peroxide Oxidation with Sustainable Low-Cost Catalysts. *Catalysts*, *12*(2), 238. https://doi.org/10.3390/catal12020238

de Jesus Silva, A. J., Contreras, M. M., Nascimento, C. R., & da Costa, M. F. (2020). Kinetics of thermal degradation and lifetime study of poly(vinylidene fluoride) (PVDF) subjected to bioethanol fuel accelerated aging. *Heliyon*, *6*(7). https://doi.org/10.1016/j.heliyon.2020.e04573

Diaz De Tuesta, J. L., Saviotti, M. C., Roman, F. F., Pantuzza, G. F., Sartori, H. J. F., Shinibekova, A., Kalmakhanova, M. S., Massalimova, B. K., Pietrobelli, J. M. T. A., Lenzi, G. G., & Gomes, H. T. (2021). Assisted hydrothermal carbonization of agroindustrial byproducts as effective step in the production of activated carbon catalysts for wet peroxide oxidation of micro-pollutants. *Journal of Environmental Chemical Engineering*, *9*(1), 105004. https://doi.org/10.1016/J.JECE.2020.105004

Diaz de Tuesta, J. L., Silva, A. S., Roman, F. F., Sanches, L. F., da Silva, F. A., Pereira, A. I., Silva, A. M. T., Faria, J. L., & Gomes, H. T. (2023). Polyolefin-derived carbon nanotubes as magnetic catalysts for wet peroxide oxidation of paracetamol in aqueous solutions. *Catalysis Today*, *419*, 114162. https://doi.org/10.1016/J.CATTOD.2023.114162

Feng, W., Deng, Y., Yang, F., Miao, Q., & Ngien, S. K. (2023). Systematic Review of Contaminants of Emerging Concern (CECs): Distribution, Risks, and Implications for Water Quality and Health. *Water*, *15*, 3922. https://doi.org/10.3390/w15223922

FENT, K., WESTON, A., & CAMINADA, D. (2006). Ecotoxicology of human pharmaceuticals. *Aquatic Toxicology*, *76*(2), 122–159. https://doi.org/10.1016/j.aquatox.2005.09.009

Fenton, H. J. H. (1894). LXXIII.—Oxidation of tartaric acid in presence of iron. *J. Chem. Soc., Trans.*, *65*(0), 899–910. https://doi.org/10.1039/CT8946500899

Gayatri, R., Fizal, A. N. S., Yuliwati, E., Zailani, M. Z., Jaafar, J., Hossain, M. S., Zulkifli, M., Taweepreda, W., & Ahmad Yahaya, A. N. (2024). Effect of polyvinylidene fluoride concentration in PVDF-TiO2-PVP composite membranes properties and its performance in bovine serum albumin rejection. *Case Studies in Chemical and Environmental Engineering*, *9*. https://doi.org/10.1016/j.cscee.2024.100620

Guo, Z., Xu, X., Xiang, Y., Lu, S., & Jiang, S. P. (2015). New anhydrous proton exchange membranes for high-temperature fuel cells based on PVDF–PVP blended polymers. *Journal of Materials Chemistry A*, *3*(1), 148–155. https://doi.org/10.1039/C4TA04952G

Hardell, E., Kärrman, A., van Bavel, B., Bao, J., Carlberg, M., & Hardell, L. (2014). Case–control study on perfluorinated alkyl acids (PFAAs) and the risk of prostate cancer. *Environment International*, *63*, 35–39. https://doi.org/10.1016/j.envint.2013.10.005

Ihsanullah. (2019). Carbon nanotube membranes for water purification: Developments, challenges, and prospects for the future. *Separation and Purification Technology*, *209*, 307–337. https://doi.org/10.1016/J.SEPPUR.2018.07.043

Ismail, A. F., Goh, P. S., Sanip, S. M., & Aziz, M. (2009). Transport and separation properties of carbon nanotube-mixed matrix membrane. *Separation and Purification Technology*, *70*(1), 12–26. https://doi.org/10.1016/J.SEPPUR.2009.09.002

Jehanno, C., Alty, J. W., Roosen, M., De Meester, S., Dove, A. P., Chen, E. Y.-X., Leibfarth, F. A., & Sardon, H. (2022). Critical advances and future opportunities in upcycling commodity polymers. *Nature*, *603*, 803–814. https://doi.org/10.1038/s41586-021-04350-0

Ji, C., Hou, J., & Chen, V. (2016). Cross-linked carbon nanotubes-based biocatalytic membranes for micro-pollutants degradation: Performance, stability, and regeneration. *Journal of Membrane Science*, *520*, 869–880. https://doi.org/10.1016/j.memsci.2016.08.056

Khan, F. S. A., Mubarak, N. M., Tan, Y. H., Khalid, M., Karri, R. R., Walvekar, R., Abdullah, E. C., Nizamuddin, S., & Mazari, S. A. (2021). A comprehensive review on magnetic carbon nanotubes and carbon nanotube-based buckypaper for removal of heavy metals and dyes. *Journal of Hazardous Materials*, *413*, 125375. https://doi.org/10.1016/J.JHAZMAT.2021.125375

Kourde-Hanafi, Y., Loulergue, P., Szymczyk, A., Van der Bruggen, B., Nachtnebel, M., Rabiller-Baudry, M., Audic, J. L., Pölt, P., & Baddari, K. (2017). Influence of PVP content

on degradation of PES/PVP membranes: Insights from characterization of membranes with controlled composition. *Journal of Membrane Science*, *533*, 261–269. https://doi.org/10.1016/J.MEMSCI.2017.03.050

Lee, S., Shin, S.-J., Baek, H., Choi, Y., Hyun, K., Seo, M., Kim, K., Koh, D.-Y., Kim, H., & Choi, M. (2020). *Dynamic metal-polymer interaction for the design of chemoselective and long-lived hydrogenation catalysts*. https://www.science.org

Lee, Y., Cho, J., Sohn, J., & Kim, C. (2023). Health Effects of Microplastic Exposures: Current Issues and Perspectives in South Korea. *Yonsei Medical Journal*, *64*(5), 301. https://doi.org/10.3349/ymj.2023.0048

Li, Y., Qi, J., Zhang, W., Zhang, M., & Li, J. (2019). Fabrication of polyvinylidene fluoride-derived porous carbon heterostructure with inserted carbon nanotube via phase-inversion coupled with annealing for capacitive deionization application. *Journal of Colloid and Interface Science*, *554*, 353–361. https://doi.org/10.1016/j.jcis.2019.06.094

Lin, S.-S., & Gurol, M. D. (1998). Catalytic Decomposition of Hydrogen Peroxide on Iron Oxide: Kinetics, Mechanism, and Implications. *Environmental Science & Technology*, *32*(10), 1417–1423. https://doi.org/10.1021/es970648k

Lindsey, M. E., & Tarr, M. A. (2000). Inhibition of Hydroxyl Radical Reaction with Aromatics by Dissolved Natural Organic Matter. *Environmental Science & Technology*, *34*(3), 444–449. https://doi.org/10.1021/es990457c

Liu, J., Yang, H., Gosling, S. N., Kummu, M., Flörke, M., Pfister, S., Hanasaki, N., Wada, Y., Zhang, X., Zheng, C., Alcamo, J., & Oki, T. (2017). Water scarcity assessments in the past, present, and future. *Earth's Future*, *5*(6), 545–559. https://doi.org/10.1002/2016EF000518

Lu, J., Dong, W., Ji, Y., Kong, D., & Huang, Q. (2016). Natural Organic Matter Exposed to Sulfate Radicals Increases Its Potential to Form Halogenated Disinfection Byproducts. *Environmental Science & Technology*, *50*(10), 5060–5067. https://doi.org/10.1021/acs.est.6b00327

Lu, N., Lin, H., Li, G., Wang, J., Han, Q., & Liu, F. (2021). ZIF-67 derived nanofibrous catalytic membranes for ultrafast removal of antibiotics under flow-through filtration via non-radical dominated pathway. *Journal of Membrane Science*, *639*, 119782. https://doi.org/10.1016/j.memsci.2021.119782

Luo, Y., Guo, W., Ngo, H. H., Nghiem, L. D., Hai, F. I., Zhang, J., Liang, S., & Wang, X. C. (2014). A review on the occurrence of micropollutants in the aquatic environment and

their fate and removal during wastewater treatment. *Science of The Total Environment*, *473–474*, 619–641. https://doi.org/10.1016/j.scitotenv.2013.12.065

Ly, Q. V., Cui, L., Asif, M. B., Khan, W., Nghiem, L. D., Hwang, Y., & Zhang, Z. (2023). Membrane-based nanoconfined heterogeneous catalysis for water purification: A critical review☆. *Water Research*, *230*, 119577. https://doi.org/10.1016/J.WATRES.2023.119577

Ma, H., Feng, G., Zhang, X., Song, C., Xu, R., Shi, Y., Wang, P., Xu, Z., Wang, G., Fan, X., & Pan, Z. (2024). New insights into Co3O4-carbon nanotube membrane for enhanced water purification: Regulated peroxymonosulfate activation mechanism via nanoconfinement. *Chemosphere*, *347*, 140698. https://doi.org/10.1016/j.chemosphere.2023.140698

Ma, H., Wang, G., Miao, Z., Dong, X., & Zhang, X. (2020). Integration of membrane filtration and peroxymonosulfate activation on CNT@nitrogen doped carbon/Al2O3 membrane for enhanced water treatment: Insight into the synergistic mechanism. *Separation and Purification Technology*, *252*, 117479. https://doi.org/10.1016/j.seppur.2020.117479

Marbelia, L., Bilad, M. R., & Vankelecom, I. F. J. (2019). Gradual PVP leaching from PVDF/PVP blend membranes and its effects on membrane fouling in membrane bioreactors. *Separation and Purification Technology*, *213*, 276–282. https://doi.org/10.1016/J.SEPPUR.2018.12.045

Mavukkandy, M. O., Zaib, Q., & Arafat, H. A. (2018). CNT/PVP blend PVDF membranes for the removal of organic pollutants from simulated treated wastewater effluent. *Journal of Environmental Chemical Engineering*, *6*(5), 6733–6740. https://doi.org/10.1016/j.jece.2018.10.029

Mishra, S., Kumaran, K. T., Sivakumaran, R., Pandian, S. P., & Kundu, S. (2016). Synthesis of PVDF/CNT and their functionalized composites for studying their electrical properties to analyze their applicability in actuation & sensing. *Colloids and Surfaces A: Physicochemical and Engineering Aspects*, *509*, 684–696. https://doi.org/10.1016/j.colsurfa.2016.09.007

Molnár, Á., & Papp, A. (2017). Catalyst recycling—A survey of recent progress and current status. *Coordination Chemistry Reviews*, *349*, 1–65. https://doi.org/10.1016/J.CCR.2017.08.011

Mompelat, S., Le Bot, B., & Thomas, O. (2009). Occurrence and fate of pharmaceutical products and by-products, from resource to drinking water. *Environment International*, *35*(5), 803–814. https://doi.org/10.1016/j.envint.2008.10.008

Ng, L. Y., Mohammad, A. W., Leo, C. P., & Hilal, N. (2013). Polymeric membranes incorporated with metal/metal oxide nanoparticles: A comprehensive review. *Desalination*, *308*, 15–33. https://doi.org/10.1016/J.DESAL.2010.11.033

Nidheesh, P. V. (2015). Heterogeneous Fenton catalysts for the abatement of organic pollutants from aqueous solution: a review. *RSC Advances*, *5*(51), 40552–40577. https://doi.org/10.1039/C5RA02023A

Nieto-Sandoval, J., Torres-Pinto, A., Pedrosa, M., Munoz, M., de Pedro, Z. M., Silva, C. G., Faria, J. L., Casas, J. A., & Silva, A. M. T. (2023). Application of g-C3N4-PVDF membrane for the photocatalytic degradation of micropollutants in continuous flow mode: Impact of water matrix. *Journal of Environmental Chemical Engineering*, *11*(5), 110586. https://doi.org/10.1016/j.jece.2023.110586

Okan, M., Aydin, H. M., & Barsbay, M. (2018). Current approaches to waste polymer utilization and minimization: a review. *Journal of Chemical Technology & Biotechnology*, *94*, 8–21. https://doi.org/10.1002/jctb.5778

OW/ORD Emerging Contaminants Workgroup. (2008). *WHITE PAPER AQUATIC LIFE CRITERIA FOR CONTAMINANTS OF EMERGING CONCERN PART I GENERAL CHALLENGES AND RECOMMENDATIONS*. https://www.epa.gov/sites/default/files/2015-08/documents/white_paper_aquatic_life_criteria_for_contaminants_of_emerging_concern_part_i_general_challenges_and_recommendations_1.pdf

Pendergast, M. M., & Hoek, E. M. V. (2011). A review of water treatment membrane nanotechnologies. *Energy & Environmental Science*, *4*(6), 1946. https://doi.org/10.1039/c0ee00541j

Peng, Y., Wang, Y., Ke, L., Dai, L., Wu, Q., Cobb, K., Zeng, Y., Zou, R., Liu, Y., & Ruan, R. (2022). A review on catalytic pyrolysis of plastic wastes to high-value products. *Energy Conversion and Management*, *254*, 115243. https://doi.org/10.1016/J.ENCONMAN.2022.115243

Prasannamedha, G., & Kumar, P. S. (2020). A review on contamination and removal of sulfamethoxazole from aqueous solution using cleaner techniques: Present and future perspective. *Journal of Cleaner Production*, *250*, 119553. https://doi.org/10.1016/j.jclepro.2019.119553

Purnawan, I., Angputra, D., Debora, S. C., Karamah, E. F., Febriasari, A., & Kartohardjono, S. (2021). Polyvinylidene Fluoride Membrane with a Polyvinylpyrrolidone Additive for Tofu Industrial Wastewater Treatment in Combination with the Coagulation–Flocculation Process. *Membranes*, *11*(12), 948. https://doi.org/10.3390/membranes11120948

Qian, F., Luo, J., Yin, H., Liu, F., Gao, S., & Gu, X. (2022). Carbonaceous composite membranes for peroxydisulfate activation to remove sulfamethoxazole in a real water matrix. *Chemosphere*, *288*, 132597. https://doi.org/10.1016/J.CHEMOSPHERE.2021.132597

Qian, F., Yin, H., Liu, F., Sheng, J., Gao, S., & Shen, Y. (2021). The in situ catalytic oxidation of sulfamethoxazole via peroxydisufate activation operated in a NG/rGO/CNTs composite membrane filtration. *Environmental Science and Pollution Research*, *28*(21), 26828–26839. https://doi.org/10.1007/s11356-021-12545-1

Ragaert, K., Delva, L., & Van Geem, K. (2017). Mechanical and chemical recycling of solid plastic waste. *Waste Management*, *69*, 24–58. https://doi.org/10.1016/j.wasman.2017.07.044

Rahim Pouran, S., Abdul Raman, A. A., & Wan Daud, W. M. A. (2014). Review on the application of modified iron oxides as heterogeneous catalysts in Fenton reactions. *Journal of Cleaner Production*, *64*, 24–35. https://doi.org/10.1016/J.JCLEPRO.2013.09.013

Rajlaxmi, Gupta, N., Behere, R. P., Layek, R. K., & Kuila, B. K. (2021). Polymer nanocomposite membranes and their application for flow catalysis and photocatalytic degradation of organic pollutants. *Materials Today Chemistry*, *22*, 100600. https://doi.org/10.1016/J.MTCHEM.2021.100600

Rana, D., & Matsuura, T. (2010). Surface Modifications for Antifouling Membranes. *Chemical Reviews*, *110*(4), 2448–2471. https://doi.org/10.1021/cr800208y

Rasheed, T., Bilal, M., Nabeel, F., Adeel, M., & Iqbal, H. M. N. (2019). Environmentally-related contaminants of high concern: Potential sources and analytical modalities for detection, quantification, and treatment. *Environment International*, *122*, 52–66. https://doi.org/10.1016/j.envint.2018.11.038

Ribeiro, R. S., Vieira, O., Fernandes, R., Roman, F. F., Diaz de Tuesta, J. L., Silva, A. M. T., & Gomes, H. T. (2022). Synthesis of low-density polyethylene derived carbon nanotubes for activation of persulfate and degradation of water organic micropollutants in continuous mode. *Journal of Environmental Management*, *308*, 114622. https://doi.org/10.1016/J.JENVMAN.2022.114622

Rizzuto, C., Pugliese, G., Bahattab, M. A., Aljlil, S. A., Drioli, E., & Tocci, E. (2018). Multiwalled carbon nanotube membranes for water purification. *Separation and Purification Technology*, *193*, 378–385. https://doi.org/10.1016/j.seppur.2017.10.025

Roman, F. F., De Grande Piccinin, L., Santos Silva, A., Diaz de Tuesta, J. L., Freitas, I. V. K., Vieira, A., Gonçalves Lenzi, G., Manuel Tavares Silva, A., Faria, J. L., & Gomes, H. T. (2023). Carbon Nanomaterials from Polyolefin Waste: Effective Catalysts for Quinoline Degradation through Catalytic Wet Peroxide Oxidation. *Catalysts*, *13*(9), 1259. https://doi.org/10.3390/catal13091259

Roman, F. F., Diaz De Tuesta, J. L., Praça, P., Silva, A. M. T., Faria, J. L., & Gomes, H. T. (2021). Hydrochars from compost derived from municipal solid waste: Production process optimization and catalytic applications. *Journal of Environmental Chemical Engineering*, *9*(1), 104888. https://doi.org/10.1016/J.JECE.2020.104888

Roman, F. F., Diaz de Tuesta, J. L., Sanches, F. K. K., Silva, A. S., Marin, P., Machado, B. F., Serp, P., Pedrosa, M., Silva, A. M. T., Faria, J. L., & Gomes, H. T. (2023). Selective denitrification of simulated oily wastewater by oxidation using Janus-structured carbon nanotubes. *Catalysis Today*, *420*, 114001. https://doi.org/10.1016/j.cattod.2023.01.008

Rouquerol, F., Rouquerol, J., & Sing, K. (1999). *Adsorption by Powders and Porous Solids*. Elsevier. https://doi.org/10.1016/B978-0-12-598920-6.X5000-3

Rout, P. R., Zhang, T. C., Bhunia, P., & Surampalli, R. Y. (2021). Treatment technologies for emerging contaminants in wastewater treatment plants: A review. *Science of The Total Environment*, *753*, 141990. https://doi.org/10.1016/j.scitotenv.2020.141990

Rueda Márquez, J., Levchuk, I., & Sillanpää, M. (2018). Application of Catalytic Wet Peroxide Oxidation for Industrial and Urban Wastewater Treatment: A Review. *Catalysts*, *8*(12), 673. https://doi.org/10.3390/catal8120673

Saljoughi, E., & Mousavi, S. M. (2012). Preparation and characterization of novel polysulfone nanofiltration membranes for removal of cadmium from contaminated water. *Separation and Purification Technology*, *90*, 22–30. https://doi.org/10.1016/J.SEPPUR.2012.02.008

Santos Silva, A., Seitovna Kalmakhanova, M., Kabykenovna Massalimova, B., G. Sgorlon, J., Jose Luis, D. de T., & T. Gomes, H. (2019). Wet Peroxide Oxidation of Paracetamol Using Acid Activated and Fe/Co-Pillared Clay Catalysts Prepared from Natural Clays. *Catalysts*, *9*(9), 705. https://doi.org/10.3390/catal9090705

Saravanan, A., Deivayanai, V. C., Kumar, P. S., Rangasamy, G., Hemavathy, R. V., Harshana, T., Gayathri, N., & Alagumalai, K. (2022). A detailed review on advanced oxidation

process in treatment of wastewater: Mechanism, challenges and future outlook. *Chemosphere*, *308*, 136524. https://doi.org/10.1016/j.chemosphere.2022.136524

Sauvé, S., & Desrosiers, M. (2014). A review of what is an emerging contaminant. *Chemistry Central Journal*, *8*. https://doi.org/10.1186/1752-153x-8-15

Schnoor, J. L. (2003). Emerging chemical contaminants. *Environmental Science & Technology*, *37*(21), 375A-375A. https://doi.org/10.1021/es032604j

Shen, L., Bian, X., Lu, X., Shi, L., Liu, Z., Chen, L., Hou, Z., & Fan, K. (2012). Preparation and characterization of ZnO/polyethersulfone (PES) hybrid membranes. *Desalination*, *293*, 21–29. https://doi.org/10.1016/J.DESAL.2012.02.019

Sheng, J., Yin, H., Qian, F., Huang, H., Gao, S., & Wang, J. (2020). Reduced graphene oxide-based composite membranes for in-situ catalytic oxidation of sulfamethoxazole operated in membrane filtration. *Separation and Purification Technology*, *236*, 116275. https://doi.org/10.1016/j.seppur.2019.116275

Sianipar, M., Kim, S. H., Khoiruddin, K., Iskandar, F., & Wenten, I. G. (2017). Functionalized carbon nanotube (CNT) membrane: progress and challenges. *RSC Advances*, *7*(81), 51175–51198. https://doi.org/10.1039/C7RA08570B

Silva, A. S., Alves, F., Diaz, L., Maria, A., Pereira, A. I., Silva, Leitão, P., & Gomes, H. T. (2022). Solving a Capacitated Waste Collection Problem Using an Open-Source Tool. *Lecture Notes in Computer Science*, 140–156. https://doi.org/10.1007/978-3-031-10562-3_11

Silva, A. S., Diaz de Tuesta, J. L., Henrique, A., Roman, F. F., Omralinov, D., Steldinger, H., Gläsel, J., Etzold, B. J. M., Silva, J. A. C., Silva, A. M. T., Pereira, A. I., & Gomes, H. T. (2024). 3D printed photopolymer derived carbon catalysts for enhanced wet peroxide oxidation. *Chemical Engineering Journal*, 156574. https://doi.org/10.1016/j.cej.2024.156574

Silva, A. S., Roman, F. F., Dias, A. V., Diaz de Tuesta, J. L., Narcizo, A., da Silva, A. P. F., Çaha, I., Deepak, F. L., Bañobre-López, M., Ferrari, A. M. C., & Gomes, H. T. (2023). Hybrid multi-core shell magnetic nanoparticles for wet peroxide oxidation of paracetamol: Application in synthetic and real matrices. *Journal of Environmental Chemical Engineering*, *11*(5), 110806. https://doi.org/10.1016/J.JECE.2023.110806

Silva, T. L. S., Morales-Torres, S., Figueiredo, J. L., & Silva, A. M. T. (2015a). Multi-walled carbon nanotube/PVDF blended membranes with sponge- and finger-like pores for direct contact membrane distillation. *Desalination*, *357*, 233–245. https://doi.org/10.1016/J.DESAL.2014.11.025

Silva, T. L. S., Morales-Torres, S., Figueiredo, J. L., & Silva, A. M. T. (2015b). Multi-walled carbon nanotube/PVDF blended membranes with sponge- and finger-like pores for direct contact membrane distillation. *Desalination*, *357*, 233–245. https://doi.org/10.1016/j.desal.2014.11.025

Singh, N., Ogunseitan, O. A., Wong, M. H., & Tang, Y. (2022). Sustainable materials alternative to petrochemical plastics pollution: A review analysis. *Sustainable Horizons*, *2*, 100016. https://doi.org/10.1016/j.horiz.2022.100016

Smith, D. L., Harris, A. D., Johnson, J. A., Silbergeld, E. K., & Morris, J. G. (2002). Animal antibiotic use has an early but important impact on the emergence of antibiotic resistance in human commensal bacteria. *Proceedings of the National Academy of Sciences*, *99*(9), 6434–6439. https://doi.org/10.1073/pnas.082188899

Smolders, K., & Franken, A. C. M. (1989). Terminology for Membrane Distillation. *Desalination*, *72*(3), 249–262. https://doi.org/10.1016/0011-9164(89)80010-4

Sun, L., & Crooks, R. M. (2000). Single Carbon Nanotube Membranes: A Well-Defined Model for Studying Mass Transport through Nanoporous Materials. *Journal of the American Chemical Society*, *122*(49), 12340–12345. https://doi.org/10.1021/ja002429w

Thomas, N., Dionysiou, D. D., & Pillai, S. C. (2021). Heterogeneous Fenton catalysts: A review of recent advances. *Journal of Hazardous Materials*, *404*, 124082. https://doi.org/10.1016/J.JHAZMAT.2020.124082

Thomas, K. V., & Hilton, M. J. (2004). The occurrence of selected human pharmaceutical compounds in UK estuaries. *Marine Pollution Bulletin*, *49*(5–6), 436–444. https://doi.org/10.1016/j.marpolbul.2004.02.028

Tijing, L. D., Woo, Y. C., Shim, W. G., He, T., Choi, J. S., Kim, S. H., & Shon, H. K. (2016). Superhydrophobic nanofiber membrane containing carbon nanotubes for high-performance direct contact membrane distillation. *Journal of Membrane Science*, *502*, 158–170. https://doi.org/10.1016/J.MEMSCI.2015.12.014

Toma, F. M., Sartorel, A., Iurlo, M., Carraro, M., Parisse, P., Maccato, C., Rapino, S., Gonzalez, B. R., Amenitsch, H., Da Ros, T., Casalis, L., Goldoni, A., Marcaccio, M., Scorrano, G., Scoles, G., Paolucci, F., Prato, M., & Bonchio, M. (2010). Efficient water oxidation at carbon nanotube–polyoxometalate electrocatalytic interfaces. *Nature Chemistry*, *2*(10), 826–831. https://doi.org/10.1038/nchem.761

Tyre, B. W., Watts, R. J., & Miller, G. C. (1991). Treatment of Four Biorefractory Contaminants in Soils Using Catalyzed Hydrogen Peroxide. *Journal of Environmental Quality*, *20*(4), 832–838. https://doi.org/10.2134/jeq1991.00472425002000040021x

Vieira, O., Ribeiro, R. S., Pedrosa, M., Lado Ribeiro, A. R., & Silva, A. M. T. (2020). Nitrogen-doped reduced graphene oxide – PVDF nanocomposite membrane for persulfate activation and degradation of water organic micropollutants. *Chemical Engineering Journal*, *402*, 126117. https://doi.org/10.1016/J.CEJ.2020.126117

Wang, C., Zheng, Q., & Yang, X. (2019). Occurrence and removal of acesulfame and sucralose in the drinking water treatment plants along the Yangtze River. *Water Supply*, *19*(5), 1305–1312. https://doi.org/10.2166/ws.2018.191

Wang, L., Li, Y., Wang, L., Wang, D., & Zhang, W. (2024). Fabrication of Fe-CoTiO3/TiO2/Ti catalytic membrane for peroxymonosulfate activation to efficient sulfamethoxazole degradation. *Separation and Purification Technology*, *339*, 126617. https://doi.org/10.1016/j.seppur.2024.126617

Wang, R., You, H., Li, Z., Zhao, J., Li, M., Zhu, J., Zhang, G., Wang, X., Leng, H., Qi, S., & Xie, B. (2024). Non-radical mediated reduced graphene oxide/polypyrrole catalytic ceramic membrane-PDS system for source control of SMX. *Chemical Engineering Journal*, *479*, 147769. https://doi.org/10.1016/j.cej.2023.147769

Wilkinson, J., Hooda, P. S., Barker, J., Barton, S., & Swinden, J. (2017). Occurrence, fate and transformation of emerging contaminants in water: An overarching review of the field. *Environmental Pollution*, *231*, 954–970. https://doi.org/10.1016/J.ENVPOL.2017.08.032

World Health Organization. (2023, September 12). *Drinking water*. https://www.who.int/news-room/fact-sheets/detail/drinking-water

Wu, M. B., Lv, Y., Yang, H. C., Liu, L. F., Zhang, X., & Xu, Z. K. (2016). Thin film composite membranes combining carbon nanotube intermediate layer and microfiltration support for high nanofiltration performances. *Journal of Membrane Science*, *515*, 238–244. https://doi.org/10.1016/J.MEMSCI.2016.05.056

Xia, X., Yan, Y., Luo, J., Liu, T., Wu, B., & Qian, F. (2023). Effects of peroxide types on the removal performance and mechanism of sulfonamide antibiotics using graphene-based catalytic membranes. *Process Safety and Environmental Protection*, *179*, 362–372. https://doi.org/10.1016/J.PSEP.2023.09.022

Xie, J., Liao, Z., Zhang, M., Ni, L., Qi, J., Wang, C., Sun, X., Wang, L., Wang, S., & Li, J. (2021). Sequential Ultrafiltration-Catalysis Membrane for Excellent Removal of Multiple Pollutants in Water. *Environmental Science & Technology*, *55*(4), 2652–2661. https://doi.org/10.1021/acs.est.0c07418

Xu, F., Wei, M., Zhang, X., Song, Y., Zhou, W., & Wang, Y. (2019). How Pore Hydrophilicity Influences Water Permeability? *Research*, *2019*. https://doi.org/10.34133/2019/2581241

Xu, L., Zhang, H., Xiong, P., Zhu, Q., Liao, C., & Jiang, G. (2021). Occurrence, fate, and risk assessment of typical tetracycline antibiotics in the aquatic environment: A review. *Science of The Total Environment*, *753*, 141975. https://doi.org/10.1016/J.SCITOTENV.2020.141975

Xu, Q., Liu, Y., Wang, Y., Song, Y., Zhao, C., & Han, L. (2022). Synergistic oxidation-filtration process of electroactive peroxydisulfate with a cathodic composite CNT-PPy/PVDF ultrafiltration membrane. *Water Research*, *210*, 117971. https://doi.org/10.1016/j.watres.2021.117971

Yadav, D., Rangabhashiyam, S., Verma, P., Singh, P., Devi, P., Kumar, P., Hussain, C. M., Gaurav, G. K., & Kumar, K. S. (2021). Environmental and health impacts of contaminants of emerging concerns: Recent treatment challenges and approaches. *Chemosphere*, *272*, 129492. https://doi.org/10.1016/j.chemosphere.2020.129492

Yang, K., Huang, L., Wang, Y., Du, Y., Tang, J., Wang, Y., Cheng, M., Zhang, Y., Kipper, M. J., Belfiore, L. A., & Wickramasinghe, S. R. (2019). Graphene oxide/nanometal composite membranes for nanofiltration: synthesis, mass transport mechanism, and applications. *New Journal of Chemistry*, *43*(7), 2846–2860. https://doi.org/10.1039/C8NJ06045B

Ye, J., Dai, J., Li, C., & Yan, Y. (2021). Lawn-like Co3O4@N-doped carbon-based catalytic self-cleaning membrane with peroxymonosulfate activation: A highly efficient singlet oxygen dominated process for sulfamethoxazole degradation. *Chemical Engineering Journal*, *421*, 127805. https://doi.org/10.1016/j.cej.2020.127805

Ye, J., Dai, J., Wang, L., Li, C., Yan, Y., & Yang, G. (2021). Investigation of catalytic self-cleaning process of multiple active species decorated macroporous PVDF membranes through peroxymonosulfate activation. *Journal of Colloid and Interface Science*, *586*, 178–189. https://doi.org/10.1016/j.jcis.2020.10.082

Ye, J., Li, C., Wang, L., Yan, Y., Wang, Y., & Dai, J. (2021). MOFs derived 3D sea urchin-like carbon frameworks loaded on PVDF membranes as PMS activator for highly efficient bisphenol A degradation. *Separation and Purification Technology*, *258*, 117669. https://doi.org/10.1016/J.SEPPUR.2020.117669

Ye, J., Wang, Y., Li, Z., Yang, D., Li, C., Yan, Y., & Dai, J. (2021). 2D confinement freestanding graphene oxide composite membranes with enriched oxygen vacancies for enhanced organic contaminants removal via peroxymonosulfate activation. *Journal of Hazardous Materials*, *417*, 126028. https://doi.org/10.1016/j.jhazmat.2021.126028

Yin, J., & Deng, B. (2015). Polymer-matrix nanocomposite membranes for water treatment. *Journal of Membrane Science*, *479*, 256–275. https://doi.org/10.1016/J.MEMSCI.2014.11.019

Yuliwati, E., & Ismail, A. F. (2011). Effect of additives concentration on the surface properties and performance of PVDF ultrafiltration membranes for refinery produced wastewater treatment. *Desalination*, *273*(1), 226–234. https://doi.org/10.1016/J.DESAL.2010.11.023

Zhang, F., Zhao, Y., Wang, D., Yan, M., Zhang, J., Zhang, P., Ding, T., Chen, L., & Chen, C. (2021). Current technologies for plastic waste treatment: A review. *Journal of Cleaner Production*, *282*, 124523. https://doi.org/10.1016/j.jclepro.2020.124523

Zhang, L. P., Liu, Z., Zhou, X. L., Zhang, C., Cai, Q. W., Xie, R., Ju, X. J., Wang, W., Faraj, Y., & Chu, L. Y. (2020). Novel composite membranes for simultaneous catalytic degradation of organic contaminants and adsorption of heavy metal ions. *Separation and Purification Technology*, *237*, 116364. https://doi.org/10.1016/J.SEPPUR.2019.116364

Zhang, L., Yang, N., Han, Y., Wang, X., Zhang, L., Sun, Y., & Jiang, B. (2021). Highly dispersed β-FeOOH nanocatalysts anchored in confined membrane pores for simultaneously improving catalytic and separation performance. *Separation and Purification Technology*, *279*, 119684. https://doi.org/10.1016/J.SEPPUR.2021.119684

Zhang, S., Hedtke, T., Zhou, X., Elimelech, M., & Kim, J.-H. (2021). Environmental Applications of Engineered Materials with Nanoconfinement. *ACS ES&T Engineering*, *1*(4), 706–724. https://doi.org/10.1021/acsestengg.1c00007

Zhang, W., Wahlgren, M., & Sivik, B. (1989). Membrane Characterization by the Contact Angle Technique. *Desalination*, *72*(3), 263–273. https://doi.org/10.1016/0011-9164(89)80011-6

Zhang, Y. S., Zhu, H. L., Yao, D., Williams, P. T., Wu, C., Xu, D., Hu, Q., Manos, G., Yu, L., Zhao, M., Shearing, P. R., & Brett, D. J. L. (2021). Thermo-chemical conversion of carbonaceous wastes for CNT and hydrogen production: A review. *Sustainable Energy and Fuels*, *5*(17), 4173–4208. https://doi.org/10.1039/d1se00619c

Zhao, X., Cheng, L., Jia, N., Wang, R., Liu, L., & Gao, C. (2020). Polyphenol-metal manipulated nanohybridization of CNT membranes with FeOOH nanorods for high-flux, antifouling and self-cleaning oil/water separation. *Journal of Membrane Science*, *600*, 117857. https://doi.org/10.1016/J.MEMSCI.2020.117857

Zhong, C., Zhang, S., Yang, S., Yuan, B., Xu, Q., Xie, Z., & Du, C. (2023). Mo and N co-doped iron biochar materials activating peroxymonosulfate for enhanced degradation of

bisphenol A: Mechanism discussion and practical application. *Chemical Engineering Journal*, *466*, 143298. https://doi.org/10.1016/j.cej.2023.143298

Zhu, W., Sun, F., Goei, R., & Zhou, Y. (2017). Facile fabrication of RGO-WO3 composites for effective visible light photocatalytic degradation of sulfamethoxazole. *Applied Catalysis B: Environmental*, *207*, 93–102. https://doi.org/10.1016/j.apcatb.2017.02.012